Physico-chemical stone-mortar compatibility of commercial stone-repair mortars of historic buildings from Paris

P. Lopez-Arce, M. Tagnit-Hammou, Beatriz Menendez, J. D. Mertz, M. Guiavarc'h, A. Kaci, S. Aggoun, A. Cousture

Physico-chemical stone-mortar compatibility of commercial stone-repair mortars of historic buildings from Paris

P. Lopez-Arce*[1,2], M. Tagnit-Hammou[2,3,4], B. Menendez[2], J.D. Mertz[3], M. Guiavarc'h[3], A. Kaci[4], S. Aggoun[4], A Cousture[4]

[1]Museo Nacional de Ciencias Naturales (CSIC), C/ Jose Gutierrez Abascal, 2, Madrid, 28024, Spain

[2]Géosciences et Environnement Cergy, GEC, Université de Cergy Pontoise, France

[3]Laboratoire de Recherche des Monuments Historiques (CRC-LRMH USR3224), 29 rue de Paris F-77420 Champs sur Marne France, France

[4]Laboratoire de Mécanique et Matériaux du Génie Civil, L2MGC, Institut des Matériaux, Université de Cergy Pontoise, F-95000 Cergy Pontoise, France

ABSTRACT

The physico-chemical compatibility of the most frequently used commercial stone-repair mortars applied to repair surface damage of a common limestone (Euville stone) employed in the basements of historic buildings from Paris was assessed. The characterization of anhydrous raw mortar materials, of stone and mortar samples collected from these buildings and laboratory specimens was carried out.

The presence of chlorides and sulfates (gypsum and mixtures of calcium and sodium sulfates) with minor amounts of nitrates in mortar samples collected from the buildings suggest an origin of salts caused by contamination/pollution coming from past restoration products and environmental pollution. The mortar containing quartz, marble aggregates, portlandite and hydraulic components (C_3S, C_2S and C_2AS) with addition of aluminosilicate micro-spherical particles with cementitious properties, and no phyllosilicates, shows a better chemical compatibility with the stone. The mechanical properties of this mortar are also closer to those of the limestone. However, some differences in the hydric properties due to their different pore systems and aesthetic features should be improved in further restoration works.

***Keywords**: stone-repair mortars; natural stone; historic buildings; compatibility; physico-chemical properties*

1. Introduction

From many architectural purposes, mortars can be used as plasters or renders covering the whole surface of walls or building facades, as bedding, jointing or pointing between stone ashlars or bricks, or even they can be used for rebuilding a decayed structure in restoration works. Some kinds of repair mortars can be applied for surface repairs of architectural surfaces. Various terms are used for these specific mortars, *stone repair mortar*, *reconstitution mortar* or *'plastic' repair mortar*, which have the same or very similar meaning to *surface repairs*, *plastic repairs*, *surface fills*, *loss compensation mortars* or *artificial stone mixtures* [1]. During restoration of heritage buildings, mortars are frequently used for the repointing of joints or for the ''plastic'' repair of stone, which are designed to fill in missing parts of stone. These mortars are moldable mortars that can be applied in situ, and sets into place by its own adhesion to the substrate [2]. From all the possible terms that can be assigned to this kind of mortars, we have chosen *'stone-repair mortar'*, since it is the clearest name for the purpose of our research, which involve mortars that have been used for repairing or reconstruction of surface damaged stone from restoration works that were carried out in historic buildings. A missing part of an original material is modelled by a new material, which is pliable when applied, and therefore can be adapted into various shapes and finished with required surface textures [1].

Repair mortars used for stone restoration are assumed to be highly compatible with historic materials in terms of physical, chemical and mechanical properties in order to assure the durability of masonry on the long term. A systematic approach for the characterization of historic mortars and materials to be repaired has been defined by

RILEM TC 167 COM which offers a valuable tool to identify mortar components, nature of binder, aggregate, additives, and their relative proportions [3,4]. Ashurst in 1990 [5] described some decision factors on surface repairs, whereas Hughes and Valek in 2003 [6] reviewed the compatibility concept. These mortars must meet a series of requirements from a Cultural Heritage preservation point of view to avoid accelerated deterioration of original material. Material compatibility between repair mortars and the original material suggests that no damage should be caused to the repaired material. For example, the incompatibility among building materials due to the combination of sulfate-bearing mortars and magnesium-rich stone and mortars applied in XVIII restoration works lead to extensive weathering on a historic Monastery (XII century) by magnesium sulfate crystallization processes [7].

Nowadays, most professionals turn to commercial pre-mixed mortars. There are many available commercial mortars ready to use in restoration works, from local and international companies. The advantage is that these are prefabricated, and the manufacturer can guarantee that the content's mix is standardized, creating the same workability and properties for each batch, with consistent composition and working properties. This is much appreciated by restoration architects and contractors [8,9]. However, this advantage can be a disadvantage as well. The specially designed mortar for one specific stone can work just for stones with the same or similar physico-chemical characteristics. Furthermore, in cases where the stone is very heterogeneous, and properties can differ greatly from one stone sample to another, the standardized process will be less successful when aiming to achieve a compatible mortar [10]. Besides, these mixes present an uncertainty about the ingredients they contain. In restoration studies using commercial mortars, aggregates are frequently added to solve the problem of stone heterogeneity [11]. In the case of ready-mixed mortars, powders

77 can simply be added with the required amount of clean water. However, is important to
78 know the physical properties of the commercial product in order to assure the
79 compatibility with the stone.

80 The selection of a binder is a starting point of the mix design as it predetermines the
81 physical and mechanical properties of the mortar mix, as well as the capacity of the mix
82 to be adapted to the appropriate form and appearance [1]. Natural Hydraulic Lime
83 mortars (NHL) are produced from a naturally occurring 'impure' limestone/chalk.
84 Typically, the impurities are those from clay minerals and other sources of alumina and
85 silica. NHL mortars have been manufactured since the XVIII century by burning these
86 limestones below the clinkering point. These NHL are able to set and harden even under
87 water, as the mechanical strength development is mainly driven by hydration.
88 Carbonation of the slaked lime contributes to the hardening process as well.

89 Hydraulic Limes mortars (HL) are produced by artificially blending calcium hydroxide,
90 calcium silicates and calcium aluminates. This is commonly achieved by blending
91 mixtures of clays and pure limestone, or calcium hydroxide with suitable pozzolanic
92 materials. Pozzolans or pozzolanic materials (fly ash, burnt clays, etc.) are reactive
93 materials that in the presence of soluble calcium hydroxide form hydrated compounds
94 which act as binders. These are often added to increase strength gain in hydrated,
95 hydraulic and natural hydraulic lime based mortars.

96 Greeks and Romans first used hydraulic lime mortars with natural pozzolans in ancient
97 times [12] and Phoenicians employed these binders in Jerusalem (10th century BC)
98 [13]. NHL was used mostly during the nineteenth century. They are nowadays used in
99 restoration of historical buildings because their chemical and physical properties are
100 similar to those of materials used by the original builders, and because they ensure the
101 development of superior mechanical properties, without having the general drawbacks

of Portland cement. NHL was the precursor of Portland cement. The main difference in the production of NHL and cement is the burning temperature. Callebaut et al. in 2001 [14] focused on the characterization of nineteenth century hydraulic restoration mortars used in the Saint Michael's Church in Leuven (Belgium), for restoring weathered mortar joints. Based on the presence of a calcium aluminosilicate (gehlenite (C_2AS)), the dominance of di-calcium silicate (larnite (C_2S)), the large amounts of portlandite (calcium hydroxide, CH), together with chemical analyses and historical sources, these hydraulic mortars were characterized as NHL mortars.

The ready-mixed mortars are available as powder materials composed of binders, aggregates and additives already packed together in appropriate ratios. The mortars preparation only consists of simple mixing operations with the correct amount of water (which is usually indicated in the technical data sheets). NHLs are frequently employed as binders in the commercial mixes because of their quick setting capability and remarkable mechanical strengths [13,15,16]. The characterization of commercial ready-mixed mortars, allows verifying their real composition and performance characteristics [17]. However, these composition and properties often differ from those declared in the technical specifications supplied by the manufacturers, finding disagreements with the composition declared by the supplier [18]. There is still a lack for testing the physical properties and durability of mortars according to European standard tests, especially in terms of compatibility with stone, and the long-term behaviour of the repaired mortar/stone interface [11].

The aim of this research is to determine the physico-chemical compatibility of the three most frequently used commercial stone-repair mortars applied to repair the surface damage of Euville stone, a common limestone used in the basements of historic buildings in Paris city.

2. Materials and methods

2.1. Characteristics of selected materials

Three commercial stone-repair mortars (Fig.1a) were selected in this research on the basis of their application on some damaged surface areas of the same type of stone, repaired due to salt crystallization processes, in different historic buildings of Paris. These buildings were repaired in the same period of time corresponding to the restoration campaign 2008-2010. The selected stone is the so-called Euville limestone (Fig.1b) that was used in the outdoor basements of the Grand Palais, Palais de la Découverte and Préfecture de Police historic buildings.

2.1.1. Stone-repair raw anhydrous mortars

Three commercial mortars, ready to mix with water according to recommendations of the manufacturers, are called in this research *Lit*, *Art* and *Alt* mortars. These are mixtures of natural and hydraulic lime mortars (NHL, HL) with or without aerial lime (CL). Lit mortar (*Lithomex Light*) is a material produced by Chaux et Enduits St. Astier (CESA, France), based on a St. Astier natural hydraulic lime binder (NHL) and it was used to repair Euville stone at the Grand Palais building (GP). According to the manufacturer, this is a pure NHL, defined as a natural lime, with hydraulic binders, sand and specific additives. According to Torney et al., 2015 [9], Lithomex mortar contains the following components (expressed as percentage of binder): calcium hydroxide 20%; hydraulic binder (Portland cement) 20%; filler (vermiculite) 5%, fine grained quartz and calcite aggregates and talc filler. The technical data sheet of *Art* mortar (*ArtoPierre TM* by Parexlanko, France) indicates that this is mainly aerial lime (CL, binder, 70% in volume) with hydraulic, mineral and organic additives and mineral pigments. Aggregates are mainly calcareous and siliceous with grains up to 1.5 mm. This mortar was used in the Palais de la Découverte building. Finally, *Alt* mortar (*Altar® Pierre* by

ECP, France) was used to repair Euville stone in the Préfecture de Police building (PP). According to the manufacturer, quartz grains, calcium carbonate, hydraulic binder, additives and mineral pigments, compose this mortar. The mineralogical and chemical composition of the three mortars, before mixing with water (anhydrous raw materials), was initially determined in this research. Then, the mineralogy and hydric and mechanical properties of hardened single mortar specimens (4x4x16 cm) were studied after 28 curing (Fig.1c).

2.1.2. Stone

Euville limestone (Oxfordian, Late Jurassic) is a crinoïdal grainstone almost completely composed of calcium carbonate (98%) with a coarse-grained texture and a syntaxial cement of calcite. The fabric was formed by an accumulation of coarse crinoïdal ossicles in submarine dunes. Accessory bivalves and spines of sea urchins are also part of the fossil fauna. The outcrops of this limestone are situated near Commercy (Département de la Meuse, France). The Euville limestone is a famous building stone in France, and also in Belgium, where it is often used in combination with Savonnières limestone and Lede stone, and it has often been used as a replacement stone in many historic buildings in several countries in the world

[19,20]. As a restoration measure, some surface areas built with this stone affected by salt crystallization processes have been repaired with several stone-repair commercial mortars. The stone specimens used in this work were supplied by ROCAMAT quarry in Euville, France. The specimens where cut parallel to the bedding with dimensions 4x4x16 cm to perform all the hydric and mechanical tests. For the water vapour permeability test cylindrical specimens 1 cm thick and 4 cm diameter were prepared.

177 *2.1.3. Stone and mortar samples collected from the historic buildings*

178 Three historic buildings from Paris city where the three types of mortars were used to
179 restore Euville stone were selected in order to collect stone and mortar samples. Two
180 small mortar samples were collected, from the Gran Palais building (GP) where
181 Lithomex mortar was used, sample Lit-GP (Fig.2a), and Préfecture de Police building
182 (PP) where Altar Pierre mortar was applied to repair the stone, sample Alt-PP (Fig.2b).
183 At the Préfecture de Police building, a small flake sample of Euville stone (Eu-GP) was
184 also collected from one area with salt crystallization decay that showed efflorescences
185 on the surface of the stone (Fig.2c). It was not possible to collect samples at the Palais
186 de la Découverte building, since the studied area corresponded to a delicate sculpted
187 stone restored with Artopierre stone-repair mortar displaying an apparent good state of
188 conservation.

189 *2.1.4. Hardened mortar specimens manufactured in the laboratory*

190 The water:powder mortar ratios were prepared in the lab, following as much as possible
191 the recommendations of the manufacturers according to their respective technical data
192 sheets. The manufacturer's preparation guidelines of Lithomex mortar state that the
193 materials should be mixed (mechanically or by hand) for between three and five
194 minutes, with water content of 4.5–5.5 L of water per 25 kg of dry material. We used 5
195 L of water (W) per 25 kg of dry material (M), i.e. W:M=0.20. In this case, the restorer
196 who used this type of mortar in the Grand Palais historical building recommended us to
197 add a handful of sand to the mixture. Since the amount of aggregate fraction between
198 1.25 and 0.63 mm in this mortar was much lower compared to the other mortars,
199 according to this information, to grain size distribution analyses and in order to obtain a
200 mortar as similar as possible to the others, 150 g of normalized sand (fraction 1.25-0.63
201 mm from Ultibat, EN 12620: 2002 + A1: 2008 [21]), was added to 2000g of raw

anhydrous mortar. To prepare Artopierre mortar, between 6 and 7 L of water per 30 kg of dry material is required according to the technical data sheet. We used 6.5 L per 30 kg of raw anhydrous mortar powder (W:M=0.22). To manufacture Altar® Pierre mortar, from 4 up to 6 volume of dry material per 1 volume of water was recommended. To prepare the specimens we used 5 volume of dry material per 1 volume of water (W:M= 0.13).

A mechanical mixture was performed in the three mortars using an industrial mixer (Controlab, France) during 4 minutes, starting at low speed rotation (62 rpm) during 1 min and finishing at high speed (125 rpm). Then, a jolting apparatus was also used according to the standard test UNE-EN 196-1:2006 [22], applying 25 blows to homogenize the mixture and avoiding the formation of air bubbles.

Eighteen mortar specimens were prepared, six with each type of mortar, two specimens for the compression-flexural test, two for water absorption under vacuum test and two for capillary-desorption test. These were prepared by molding the mixtures in rubber molds (4x4x16 cm). Besides, to carry out water vapor permeability tests, plastic moulds filled with each mortar mixture were used. These were big enough to prepare by cutting at least two circular mortar specimens (50 mm diameter x 10 mm thickness) for each type of mortar. All the specimens were demolded after two days of curing according to the standard test NF-EN 1015-11 [23].

For hardening the mortar specimens (28 days curing) we tried to simulate the average annual weather conditions of Paris. The specimens were placed in a ventilated climatic chamber with CO_2 uptake from the environment (400 ppm approx.) at 11ºC and 85% relative humidity (RH)) during 7 days. Then, RH was changed down to 65% during the next 7 days, followed by laboratory conditions in a climatic room at 20ºC and 50% RH during 14 days, under environmental CO_2 (400 ppm approx.)). The reason why RH was

227 reduced from 85% down to 65% during the 7-14 curing days was first of all, because
228 the average annual RH in Paris city was in the range 65-85 % RH approx. In a second
229 place because these commercial mortars are mixtures of hydraulic and aerial lime.
230 According to the literature [24,25], a high and a lower RH, respectively, is
231 recommended to set up suitable curing conditions. The European standard AFNOR EN
232 1015-11 [23] defines the following optimal conditions of temperature and relative
233 humidity for the curing of mortar samples in the laboratory at T=20±2 °C and
234 RH=95±5% for the first 5 days in the mold, the following 2 days removed from the
235 mold, and at T=20±2 °C and RH=65±5% for the following 21 days. So, 85-65% RH
236 and 11ºC T conditions were selected the first 14 days in order to simulate as much as
237 possible the environmental curing conditions of Paris and at the same time trying to
238 perform a laboratory test in a gradual way choosing the most suitable as possible curing
239 conditions for these type of mortars. The environmental conditions of the final 14 days
240 to reach 28 curing days had to be performed at RH 50±5%, T 20ºC in a climatic room
241 only due to availability and space reasons.

242 *2.2. Analytical techniques and experimental test methods*

243 *2.2.1. Mineralogical and chemical analyses*

244 Polarizing optical microscopy was used to study the main mineralogical constituents
245 and textures of the mortar samples collected from the buildings and the hardened single
246 mortar specimens after 28 days curing. The samples were impregnated with epoxy resin
247 mixed with blue dye to fill the porosity in order to be easily recognized under the
248 microscope with parallel nicols. The thin sections were studied with an Olympus BX50
249 polarized light microscope fitted with an Olympus digital camera.

250 X-ray diffraction (XRD) was used to determine the mineralogical composition of raw
251 anhydrous mortar samples, hardened single mortar specimens manufactured with them

252 after 28 days curing and samples collected from the buildings. Furthermore, soluble
253 fractions prepared to carry out ion chromatography analyses were left to evaporate and
254 the product was also analysed by XRD. The analyses were conducted on a Bruker D8
255 Advance diffractometer with CoKα radiation powder. The scanning conditions were 2θ
256 angles of 5–65º, scan step size 0.05º, time step 1º/s in continuous mode, and beam
257 intensity of 40 kV and 35 mA. The diffractometer worked with a CoKα radiation,
258 instead of the most common used CuKα and so there is a slight variation in the grades
259 of the 2θ peaks used to identify minerals. The identification of the mineral phases was
260 performed using the Bruker AXS DiffracPlus EVA software also used to carry out
261 semi-quantitative analyses.

262 Scanning electron microscopy (SEM) coupled with Energy dispersive X-ray
263 spectroscopy (EDS), was used to find weathering products caused by decay processes
264 and to identify the type of salt efflorescences and sub-efflorescences on the top and
265 underneath (some millimetres depth) the surface of stone and mortar fragments
266 collected from the buildings. A SEM microscope Leica S430i was used. The elemental
267 composition of some selected components from these building samples together with
268 the raw anhydrous mortar samples was determined by means of EDS semi-quantitative
269 microanalyses by means of an Bruker micro-analyser spectrometer. Nickel-sputtered
270 fragments from the samples were studied in secondary electrons mode.

271 In order to perform the chemical composition by EDS analyses of each grain size
272 fraction of the raw anhydrous mortars (aggregates and binder), the grain or particle size
273 distribution was carried out by sieving 200g approx. of each mortar according to the
274 standard test AFNOR NF-EN 1015-1 [26]. The sieve sizes that have been used are the
275 following: 1.60mm, 1.25mm, 0.63mm, 0.315mm, 0.20mm, 0.16mm, 0.080mm and
276 0.080mm. Then, the largest sizes (1.60-1.25 mm and 1.25-0.63 mm) were impregnated

277 in epoxy resin and then polished, in order to study their shape and chemical
278 composition by SEM-EDS analyses. Each grain size range of the finest fractions (from
279 0.63 down to below 0.080 mm) was pressed in small tablets and then analyzed by EDS
280 previously sputtering the samples with nickel (Ni).

281 Ion chromatography (IC) analysis was performed to quantify the soluble salts present in
282 the raw anhydrous mortars and samples collected from the buildings. Some anions (Cl^-,
283 NO^{-3}, PO_4^{2-} and SO_4^{2-}) and cations (Na^+, K^+, Mg^{2+}, Ca^{2+} and NH_4^+) were determined.
284 Approximately 0.1 g of sample was dissolved in 10 ml of Milli-Q ultrapure water and
285 placed it for 5 min in an ultrasonic bath at room temperature. The solution with the solid
286 residue was then left to settle down with a minimum rest period of 24 h. The soluble
287 salts of raw materials and samples collected from the buildings were quantified on a
288 Dionex DX-120 ion chromatograph.

289 *2.2.2. Physical tests*

290 To determine hydric and mechanical properties, together with physical characteristics
291 such as density, porosity and color parameters, the following tests were carried out in
292 the stone and mortar specimens.

293 Water absorption by capillarity was carried out to evaluate the liquid water transfer into
294 the materials. The capillary coefficients were calculated for the Euville stone and
295 hardened single mortar specimens. The standard test AFNOR NF EN 1925:1999 [27]
296 was followed; the results are expressed in $g/(m^2 \cdot s^{1/2})$ instead of $kg/(m^2 \cdot s^{1/2})$. Once
297 capillarity saturation was reached, the specimens were spun to ease the water drying
298 under laboratory conditions (45±5 % RH and 20±1ºC) and to calculate desorption
299 coefficient (water loss or evaporation) weighing the specimens at several intervals of
300 time.

301 Water vapour permeability test was carried out in the stone and mortar specimens. The
302 standard test AFNOR EN 15803:2010 [28], with wet cup was followed to calculate the
303 water vapor permeability ($Kg/(m^2s)$). External relative humidity of 50% and
304 temperature of 23ºC were achieved introducing the specimens in a climatic chamber,
305 setting these conditions during all the duration of the test.

306 Water absorption under vacuum was performed in the stone and hardened mortar
307 specimens, to determine differences on apparent density (kg/m^3), bulk density (kg/m^3),
308 and to calculate open porosity (%) as described in standard test AFNOR EN 1936:2007
309 [29].

310 Flexural strength measurements were carried out in the stone and hardened mortar
311 specimens, with a maximum load of 8 kN and load rate of 0.05 kN/S. Compression
312 strength measurements were performed in the four fragments obtained from the
313 breaking of two specimens after the flexural test. A maximum load of 250 kN and load
314 rate of 2.4 kN/S was applied until breaking, providing values equal or above 7 MPa,
315 since this is the minimum value detected by the compression cell. A Quantech 3R press
316 (Quantium^{TM}, Researchers & Realisations, France) that follows the standard test
317 AFNOR EN196-1:2006 [30] was used.

318 Total Hg-porosity and pore size distribution analysis was carried out by mercury
319 intrusion porosimetry in the stone and mortar samples collected from the building and
320 the superficial part of hardened mortar specimens manufactured in the laboratory.
321 Readings were taken at pore radius of 0.003–200 μm under measuring conditions
322 ranging from atmospheric pressure to 228 MPa on a Micromeritics Autopore IV 9500.

323 Color parameters were measured on the stone and mortar hardened specimens. L*
324 parameter, which accounts for luminosity, hue and saturation (chroma, C), a* and b*
325 coordinates (a* being the red-green parameter and b* the blue-yellow) were obtained.

Total color difference ΔE* was provided as a result of the formula $\Delta E^* = ((\Delta L^*)^2 + (\Delta a^*)^2 + (\Delta b^*)^2)^{1/2}$. Measurements were performed with a spectrophotometer Konica MINOLTA CM-2300d using the CieLab color space; standard illuminant was D65 and observer angle, 10º.

3. Results

3.1. Characterization of raw anhydrous mortars

The main mineralogical composition of Lit mortar determined by XRD is calcite, quartz, feldspar and phyllosilicates (clinochlore and talc), followed by hydraulic components, larnite (i.e. C_2S or belite), alite (C_3S) and traces of gehlenite (C_2AS). Art mortar contains mainly quartz, calcite and portlandite (i.e. CH or $Ca(OH)_2$) and hydraulic phases, di-calcium silicate (larnite) and tri-calcium silicate (alite), and traces of feldspar and calcium-aluminium silicate (gehlenite). A small hump between 10 and 15º 2θ can be observed in the XRD pattern of this mortar, which might be related to the presence of clays. Alt mortar XRD pattern shows quartz, feldspar, calcite, portlandite, larnite, alite and traces of gypsum and gehlenite (Fig.3 and Table 1).

The SEM-EDS analyses performed in several areas of mineral grains (aggregates) with sizes between 1.6-1.25 mm and 1.25 mm-0.63 mm of Lit mortar (Fig. 4a) correspond to phyllosilicates compositions (clinochlore and talc), with and without additional K, Ti and Cl only detected in the aggregates in the range between 1.6-1.25 mm (Table 2). Mineral grains of Lit mortar with sizes in the range between 1.25-0.63 mm correspond to calcite composition with some traces of Mg, Al, Si and Na (Fig. 4b). The results of these analyses performed in Art mortar show that the mineral grains in the ranges between 1.6-1.25 mm and 1.25 mm-0.63 mm are mainly, calcite, quartz (that were deposited in the bottom of the prepared epoxy specimen) and similar phyllosilicates than those present in Lit mortar (Fig.4c). By contrast, SEM-EDS analyses carried out in

351 the grain sizes between 1.60-1.25 mm and 1.25-0.63 mm of Alt mortar show that these
352 are only composed by sub-rounded and sharp calcite composition grains, which
353 partially might correspond to the marble grains added by the manufacturer (Fig.4d).
354 Some of these grains contain some fissures filled with quartz and some impurities such
355 as sodium chloride (NaCl). The composition of these largest grain size aggregates in
356 this latter mortar shows significant differences compared to the other two mortars
357 (Table 2), since Al, Mg and k are not detected and there is no Fe and Ti in the fraction
358 between 1.60-1.25 mm.

359 In the three mortars, the composition of the aggregates between 0.63 and 0.20 mm is
360 mainly siliceous (Si content between 20 and 40 wt. % approx.), and this is especially
361 marked in Alt mortar (Table 3). Below 0.20 mm the Si content greatly decreases at
362 expenses of Ca content, which especially increase in Art and Alt mortars (between 27
363 and 40 wt. % approx.). Besides this, the main difference among the three mortars is the
364 Na content in Alt mortar which increases with the decrease of grain size (except in the
365 range between 0.16 and 0.080 mm), from 4 wt. % (between 0.63-0.315 mm) up to 33
366 wt. % (below 0.080 mm).

367 Ion chromatography analyses show that none of the anhydrous mortars display nitrates
368 in their composition (Table 4). However, the three have a slight amount of chlorides
369 (circa 5 ppm). The only one displaying soluble sulfates is Lit mortar (23 ppm approx.).
370 The concentration in bulk material (wt.%) of the identified total soluble salts (cations
371 and anions) represents very low percentages in Lit and Alt mortars (2 %) and slightly
372 higher values in Art mortar (circa 5 %). There is a high amount of soluble Ca^{2+} in the
373 three mortars and this is especially high in Art mortar. No nitrates or phosphates, neither
374 ammonium have been detected in these samples.

375

3.2. Mortars and stone flake samples collected from the buildings

Petrography of mortars thin sections performed under optical light microscopy shows that Lit mortar from the Grand Palais building has a large quantity of rounded esparitic calcite and quartz grains with submillimetric sizes, together with some micas and many phyllosilicates embedded in a scarce micritic matrix composed by a mixture of calcite and clays. The ratio binder:aggregate is approximately 1:4 (Fig. 5a and 5b). Feldspar grains show up with a high degree of cracking at the surface of the mortar that was in contact with the surrounded environment where the sample was collected. Porosity is mainly fissural and surrounds the mineral grains and goes through the clay minerals and through the matrix. Large pores inside the matrix are associated in some areas to the phyllosilicates showing signs of weathering (Fig.5c and 5d). Thin sections of Alt mortar from Préfecture de Police building also show a high amount of calcite crystals inside sharp fragments of fossiliferous micritic and esparitic limestone rocks, bioclasts and marble fragments of millimetric size. Abundant smaller feldspar and subhedral quartz grains with cement as syntaxial overgrowths are also embedded in a dense dark matrix. The ratio binder:aggregate is approximately 1:3 (Fig.5e and 5f). Small rounded (circa 50 μm) and larger sub-rounded pores (between 200 and 400 μm), together with small spherical particles (circa 50 μm) are present inside this matrix. Some of these particles seem to be stuffed with an amorphous gel, being difficult to distinguish them from the matrix, while many others are empty and filled now with the dyed blue resin used to mark the porosity of the mortar samples (Fig.5g and 5h).

The XRD pattern of Lit mortar collected from the Grand Palais building (Lit-GP), displays the same mineralogy than the obtained in the raw anhydrous mortar, with the exception of the presence of muscovite ($K(Li,Al)_2(Si_3AlO_{10})(OH)_2$) and gypsum ($CaSO_4 \cdot 2H_2O$) and the absence of larnite (C_2S) and alite (C_3S) (Fig.6). The semi-

401 quantitative (%) analyses show different concentrations in all the identified phases
402 compared to its corresponding raw material (Table 1). The mineralogy of the salts
403 precipitated from the soluble fraction of Lit mortar prepared to carry out the ion
404 chromatography analyses, that were left to evaporate (Lit-GP-sf), shows an increase of
405 gypsum peaks and the appearance of halite (NaCl). Some residues of non-soluble
406 fraction (quartz, calcite, clinochlore and talc) are also detected.

407 The XRD pattern of Alt mortar collected from the Préfecture de Police building (Alt-
408 PP) also shows the same mineralogy than the obtained in the anhydrous raw material,
409 with the exception of no detection of gypsum, the absence of alite (C_3S) and the
410 presence of a minor amount of larnite (C_2S). The semi-quantitative (%) analyses also
411 show different concentrations in all the identified phases compared to its corresponding
412 raw material, especially in the amount of portlandite (Fig.6). No salts are identified in
413 the mortar sample collected from this building and neither in the precipitated soluble
414 fraction. The XRD of Euville stone flake (soluble fraction after evaporation) shows
415 gypsum, halite and traces potassium-sodium sulfate.

416 The SEM-EDS analyses of the surface of Lit mortar from the Gran Palais, mainly shows
417 Ca, Mg, C, O, Si and Al as the main components present in all the analyzed zones.
418 Underneath the surface it shows aggregates of quartz and mainly Si and Ca (i.e. calcium
419 silicates) as the composition of the binder. There are zones with large amounts of salts
420 composed by S and Ca (i.e. gypsum) and Na and Cl (i.e. sodium chloride) (Fig.7a, zone
421 1 and zone 2, respectively). A great number of phyllosilicates is also observed.

422 On the surface of Alt mortar samples from Préfecture de Police building, Si, Ca, Al, C,
423 O, Na and Cl are the main components, with variable amounts in all the analyzed zones.
424 There are zones with large amounts of Na and Cl (sodium chloride). Underneath the
425 surface of Alt mortar, the main composition of the binder is Si and Ca, with Al, C and

O. Many micron-size spherical particles can be observed, some of them seem to be cracked and empty and others seem to be filled with a “viscous” phase. The EDS analyses show a thin external part mainly composed by aluminosilicates (Fig.7b, zone 1), which might correspond to mullite ($2Al_2O_3 \cdot SiO_2$). Some of them display also Ca in the external part. The analyses of the interior part of these particles show a high increase in Ca and minor amounts of Na and Mg (Fig. 7b, zone 2). Aggregates of marble fragments can also be observed. However, they display low amount of C and some Al in their composition. The EDS analyses of Alt mortar (external and internal parts) indicate the presence of salts (sodium chloride) together with aluminosilicates, calcium silicates, calcium aluminosilicates, calcium carbonate and silicon oxides.

The surface of Euville stone flake displays salt efflorescences containing S, K, Ca and Na (Fig.7c, surface zone). Some millimeters depth from the surface, the SEM images show sub-efflorescences of sodium and calcium sulfate crystals mixed together, which might corresponds to thenardite and gypsum, respectively (Fig. 7c, interior zone).

Table 5 shows the ion chromatography results of soluble salts present in the samples collected from the buildings. There is a large amount of sulfates in Lit mortar sample collected from Grand Palais, above 100 ppm. The amount of sulfates in Alt mortar sample from Préfecture de Police is much lower (21 ppm). The amount of chlorides is also lower in Alt mortar (11 ppm) compared to Lit mortar (circa 30 ppm). The presence of nitrates is detected in both mortars, circa 25 ppm in Lit mortar and circa 34 ppm in Alt mortar. The concentration in bulk material (wt.%) indicates higher percentages of total soluble salts (cations and anions) in Lit mortar compared to Alt mortar, even though these values are very small in both cases. The ion chromatography analyses of the stone flake collected from the Préfecture Police building show a concentration of sulfates and chlorides of 984 ppm and 17 ppm, respectively. Nitrates were not detected

in this sample. The content of soluble K^+ and Ca^{2+} in this sample is especially high. The concentration of salts in bulk material in this sample (that contained efflorescences) is much higher compared to the mortars (circa 12 wt.%). No phosphates or ammonium were detected in these samples.

Figure 8 shows the pore size distribution obtained by mercury intrusion porosimetry in the mortars collected from the buildings, which have a very different total porosity accessible to mercury. Lit mortar sample has a higher total Hg-porosity (circa 26%) compared to Alt mortar (circa 16%). The pore size distribution of the former is mainly polymodal with the highest volume of pores with radius in the range between 0.1 μm and 3 μm (Fig.8a). It displays also larger pores with radius in the range between 3 and 10 μm, and smaller pores with radius below 0.02 μm. Alt mortar porosimetry curve is mainly bimodal with most of their pores with radius in the range between 0.5 and 1 μm and pores below 0.01 μm (Fig.8b).

3.3. Stone and hardened mortar specimens manufactured in the lab

3.3.1. Mineralogical characterization

Thin sections of Lit and Alt hardened mortars under optical light microscopy (Fig.9a-b and Fig.9c-d respectively) show a great similitude with those samples collected from the buildings (Fig. 5). The matrix or binder of the laboratory hardened mortars show lighter colors and rounded pores (500 μm approx.) that could be related with a lower degree of maturation and the lack of exposition to weathering agents. The small rounded pores (around 50 μm) that were observed in the thin sections of Alt mortar from the building are not observed in the same mortar manufactured at the lab. In the latter, there are many spherical particles circa 50 μm embedded in the matrix that can be clearly distinguished from it by a thin rim filled with the resin (no blue dyed), which indicate

475 spherical hollow not connected particles. The thin sections of Art mortar show
476 aggregates of calcite, quartz, feldspars and many phyllosilicates with some micas. There
477 are many small rounded pores (filled and not filled with the blue dye, which would
478 represent open and non-connected porosity), together with fissural porosity going
479 through the matrix, and intra particle porosity associated to phyllosilicates (Fig.9e and
480 9f). Euville stone thin sections show a larger size of the mineral grains compared to the
481 mortars (Fig.9g and 9h). Bioclasts, such as crinoids, sea urchins, brachiopods, coral
482 fragments and pellets can be easily recognized. Syntaxial calcite cement occupies a
483 large part of the stone that gives rise to the cohesion of the grains. Shell fragments are
484 filled with calcite sparitic cement and their edges are surrounded by sparitic and micritic
485 cement in some areas. Heterogeneous macro-pores are left by the syntaxial overgrowth
486 while micro-pores are mainly intra-particle or located between the micrite and sparite
487 crystals around shell fragments. Some quartz and clays can be also observed in minor
488 amounts.

489 The XRD patterns of the 28 days hardened mortars manufactured in the laboratory
490 reveal the development or increase of portlandite, the decrease of larnite (C_2S) and the
491 disappearance of alite (C_3S) regarding to the analyses carried out in their corresponding
492 raw anhydrous mortars (Table 1 and Fig.10). In all the mortars the decrease of larnite
493 peaks is evident together with the improvement of crystallinity of portlandite (CH)
494 reflected by the sharpness and intensity increase of the main CH peak .

495 *3.3.2. Physical characterization*

496 A complete characterisation of the physical properties of Euville stone and the 28 days
497 hardened mortar specimens has been done.

498 Concerning liquid water transfer (Table 6) it can be seen how Lit mortar specimens
499 display a very low capillarity coefficient compare to the rest of mortar specimens. The

500 total amount of water at the end of the tests (Fig. 11) is also much lower than for the
501 others mortars (Fig. 11a) and Euville stone (Fig.11c). In Lit mortar specimens,
502 evaporation (water loss) is also slower than in the rest of materials but the difference is
503 less important than for capillarity (Fig.11b). Art mortar specimens get more water than
504 the others and in a very quick way. Alt mortar and Euville stone have a similar
505 behaviour during the capillarity test: similar velocity and same water content at the end
506 of the test, but Euville stone losses the water by evaporation much faster than this and
507 the other mortars (Fig.11d). At the end of the evaporation test Euville stone has lost all
508 the water taken during the capillarity test. Water vapour permeability is also quite
509 similar in Alt mortar and Euville stone. Art mortar shows the highest water vapour
510 permeability values while permeability of Lit mortar is in between the values obtained
511 in Art and Alt mortars and Euville stone. We can notice that water vapour permeability
512 and porosity are directly related; roughly we can consider that an x10E11 factor exists
513 between vapour permeability and open porosity.

514 Comparing the values of open water porosity and mercury porosity values (Table 7) it
515 can be observed that the former porosity is between 10 and 20% higher than the latter,
516 in all the materials except Lit mortar. For Lit mortar, mercury porosity is slightly higher
517 than water porosity. Bulk density corresponds to the density of "minerals" that form
518 part of these materials. Euville stone specimens have the highest bulk density
519 (2.55g/cm^3), slightly lower than the calcite density (2.71 g/cm^3). Comparing the three
520 mortars, Lit mortar has the highest bulk density, followed by Alt and Art mortars. This
521 can be explained by its mineralogical composition. Apparent density depends on
522 porosity and bulk density, showing that Euville stone is more "compacted" than the
523 mortars. Concerning the mortars, Alt mortar has the highest apparent density, followed
524 by Lit and Art mortars. Apparent density is inversely related to water open porosity, i.e.

525 the highest the open porosity the lower the apparent density. Apparent density values
526 obtained by mercury porosimetry correspond very well to values obtained by water
527 immersion test. For bulk density it can be observed the same pattern than for porosity,
528 mercury porosimetry values are slightly lower than water porosity values, except for Lit
529 mortar specimens.

530 Pore size distribution (PSD) is different for all the samples, where it can be considered
531 two different cases. First, Lit and Art mortars display a clear bimodal PSD which is
532 quite similar, with an average pore radius circa 0.10µm for Lit and 0.13µm for Art
533 mortar; median pore radius are about 0.5 µm for Lit and 0.4 µm for Art, in both cases
534 the median radius is higher than average radius. Alt mortar and Euville stone show
535 average pore radius higher than median radius, 0.04µm and 0.01µm for Alt mortar
536 respectively, and 1.4µm and 0.8µm for Euville stone, respectively. Euville limestone
537 has larger pores than the mortars, above 10 µm (Fig.12). In all the mortars median
538 radius is smaller than the modal pick, indicating a bias to the smaller pores; Euville
539 limestone has a median bigger than the mode, reflecting the bias to the biggest pores.
540 Difference between mode and median is smaller in Euville stone than in mortars,
541 because it has a more symmetrical PSD. This difference is more important in Alt mortar
542 and we can observe a big “tail” in the distribution that takes place in the range of
543 smallest pores.

544 The comparison between capillarity coefficients and pore size distributions for Art and
545 Alt mortars and Euville limestone, indicates a direct relation between capillarity
546 coefficients and pore sizes. In order to avoid the effect of water volume absorbed during
547 the capillarity test, the capillarity coefficient (C) has been divided by the porosity values
548 (P), in this way, the obtained values correspond to the median pore radius values of
549 0.82µm (Euville), 0.41µm (Art) and 0.01µm (Alt) (Table 7). A linear regression among

these values gives an equation C/P = 1.2461 x (median pore radius) + 1.9591, with a regression coefficient of $R^2 = 0.9438$.

Results of mechanical tests obtained in these stone and hardened mortar specimens are presented in Table 8. Art mortar has a mechanical behaviour different from the others, since the flexural and compression strengths are much lower than the obtained in the other mortars. The experimental resolution of the mechanical tests machine used is not adapted to Art mortar specimens. So if this mortar is not considered, a very good linear regression between flexural strength and apparent density ($R^2 = 0.999$) can be obtained.

The spectrocolorimetry results are compiled in Table 9. The highest total color difference (ΔE^*) between each mortar and Euville stone is obtained in Art mortar (circa 8), followed by Alt (circa 5) and Lit mortar that shows the lowest differences (circa 3).

4. **Discussion**

4.1. Chemical and mineralogical characterization

The original chemical and mineralogical composition of the raw anhydrous mortars exert a great influence on their final physico-chemical properties in a short and in a longer term, and hence on the compatibility with the stone to be repaired and their durability [31]. Quartz, calcite, feldspar and larnite/belite, alite and traces of gehlenite (hydraulic components, C_2S, C_3S and C_2As, respectivelly) are present in the three raw anhydrous mortars (Fig.3 and Table 1). The main difference in their mineralogy determined is the absence of phyllosilicates in Alt mortar and the absence of aerial lime (portlandite) in Lit mortar. The former contains high quantity of portlandite and calcium and aluminosilicates (larnite, alite and gehlenite) while the latter has abundant phyllosilicates (clinochlore and talc) and no portlandite. Art mortar composition is in between the two other mortars, with portlandite, larnite and alite, and some phyllosilicates (vermiculite, which was only possible to identify in the XRD and

575 petrography of the 28 days hardened mortars and not in the XRD of the raw anhydrous
576 materials (although the presence of phyllosilicates was inferred by a small hump
577 between 10 and 15 º2θ in the XRD pattern). The identified soluble salts determined by
578 ion chromatography represent insignificant values in the concentration in bulk material
579 (wt.%), around 2 % in Lit and Alt mortar, which should not represent a salt
580 crystallization problem or development of salt efflorescences, and a slightly higher
581 content in Art mortar (5%). However, is important to take into account that these
582 percentages include a high concentration of soluble calcium (Ca^{2+}), which could be
583 combined with other anions that were no possible to identify with the chromatographic
584 column used in these analyses. Soluble calcium combined with other anions such as
585 carbonates (CO_3^{2-}), silicates (SiO_4^{4-}) or hydroxides (OH^-) could form part of these
586 mortars, especially in Art mortar with a higher concentration of soluble Ca^{2+} (Table 4).
587 The characterization of stone and mortar samples collected from the historic buildings
588 has been useful to know the current composition and texture of the mortars set under
589 real conditions and five years of hardening and to study the weathering products causing
590 decay in these materials. The identification of salt minerals by XRD, SEM-EDX and the
591 quantification of soluble salts by ion chromatography have served to plan the
592 accelerated ageing test to assess the durability of stone-mortar specimens in the lab [31].
593 The presence of chlorides and sulfates (gypsum and mixtures of calcium and sodium
594 sulfates) with minor amounts of nitrates suggest an origin of salts caused by
595 contamination/pollution coming from past restoration products and environmental
596 pollution (Fig.6, Fig.7 and Table 5).
597 Lit mortar, classified as a NHL according to the manufacturer, displays a high amount
598 of phyllosilicates that could have favour cracking of the mortar at the interface stone-
599 mortar observed at the Grand Palais building when mortar samples were collected

600 (Fig.2). In the frame of Dimppa Project [32] on site measurements with non-destructive
601 techniques were carried out in this building in the same type of mortar and stone. High
602 salt index values were found at the interface between Lit mortar and Euville stone,
603 together with large differences on the thermal behaviour between both materials.
604 Restorers frequently use clay rich sands because they can increase workability and
605 matching the right colour for the restoration mortar. However, the main effect of clay
606 fines (<63 μm) in aggregates is an increase of the water demand, due to their high
607 surface area, for a constant mortar consistency that gives rise to a poor quality mortar
608 [33]. However, it does not mean that NHL produce bad results in this type of restoration
609 works, it just depends on the type, proportion and grain size of the minerals in the
610 original composition and the compatibility with the stone substrate. The characterization
611 of original mortars and plasters from Crete was carried out with the evaluation of the
612 repairs prepared with NHL as binding material, siliceous sand and crushed brick as
613 aggregates [34]. After three years of intervention with these NHL-based mortars and
614 plasters, macroscopic survey and analyses on the applied materials revealed that no
615 cracks or release of soluble salts occurred.

616 In this case, this NHL mortar collected from the Grand Palais building (Lit mortar) has
617 a higher total porosity and a polymodal pore size distribution, compared to the HL
618 mortar collected at the Préfecture de Police building (Alt mortar). The hardened mortar
619 specimens manufactured and cured during 28 days in the lab, show the presence of
620 fissural porosity mainly through the matrix of Lit mortar (Fig.9). The XRD patterns of
621 all the hardened mortars manufactured in the laboratory (Fig.10) reveal the development
622 of portlandite (CH) in Lit mortar or its increase in Art and Alt mortars, the decrease of
623 larnite (C_2S) and the disappearance of alite (C_3S) regarding to the analyses carried out
624 in their corresponding anhydrous raw materials (Fig.3). In Art mortar the decrease of

625 C_2S peaks can be observed together with the improvement of crystallinity of CH peaks
626 and the appearance of vermiculite or clinochlore peaks. In Alt and Lit mortars there is
627 also a decrease in C_2S and disappearance of C_3S peaks and the improvement of
628 crystallinity of portladite reflected by the sharpness and intensity increase of the main
629 portlandite (CH) peak. This is explained because the hydration of C_3S and C_2S produce
630 CH and some of new CH amount can also crystallize, inside of the CSH (calcium
631 silicate hydrates) structure being well sheltered [13]. This fact has been related to the
632 improvement of mortar strength [35-37], while C_3S contributes to the strength at early
633 ages, C_2S and the carbonation process give their strengths at long term [13].

634 The addition of micro spherical aluminosilicate particles (diameter of 50 μm) similar to
635 fly ash (FA), into Alt mortar was confirmed through the SEM-EDS analyses, where
636 these appear empty, cracked or filled with a viscous gel rich in calcium (Fig.7b). Using
637 fly ash with small and spherical shape in mortar or concrete can reduce water demand of
638 the mixtures [38]. Chemically, fly ash has pozzolanic activity, which is attributed to the
639 presence of SiO_2 and Al_2O_3. It reacts with calcium hydroxide (CH) during cement
640 hydration, to form additional calcium silicate hydrate (CSH), calcium aluminate hydrate
641 (CAH) [39] and calcium aluminosilicate (CAS) gels. This can also be explained by the
642 denser and darker color matrix of Alt mortar under light optical microscopy and higher
643 physico-chemical compatibility with Euville stone compared the other mortars. The
644 addition of these spherical micro-capsules, seem to have been added to Alt mortar
645 mixture in order to improve the mechanical properties acting as a self-healing
646 cementitious material. Besides these spherical particles, the abundant circular air voids
647 uniformly distributed in the binder's matrix of both Alt and Art mortars, that creates an
648 apparently high visible porosity is most probably due to the addition of an air
649 entrainment agent in the mortar mix [17].

650 The binder:aggregate ratio between 1:3 and 1:4 of the mortars from the buildings
651 (Fig.5) is in agreement with ratios of similar mortars used in restoration works of
652 historic buildings in other countries. Pecchioni et al. in 2005 [40] study some Florentine
653 Palaces (Italy) and the analytical results show that the aggregates were composed by
654 silicate sand and the binder/aggregate ratio ranged between 1:1 and 1:3, with presence
655 of larnite.

656 Even though petrography and physical properties of Euville stone have been deeply
657 studied [19,20], due to its high heterogeneity, the petrography and physical properties of
658 the specific specimens used in this research was carried to study the compatibility with
659 the stone-commercial mortars. The heterogeneity of this limestone has been also
660 observed through on-site measurements on historic buildings and in-lab measurements
661 with non-destructive techniques [32].

662 *4.2. Physical characterization*

663 In this research we have characterized water (liquid and vapour) transfer through
664 mortars by means of imbibition properties (capillarity rise), evaporation (desorption
665 test) end water vapour permeability. The results show that capillarity imbibition,
666 evaporation and vapour permeability values of 28 hardened Art mortar specimens are
667 higher than in the others mortars. The reason is the high porosity of this mortar with
668 pore sizes slightly larger than the others. Alt mortar specimens have physical properties
669 close to those of Euville limestone but with a capillarity coefficient lower than the stone
670 and a very low evaporation degree.

671 The mechanical behaviour of Lit and Art mortar specimens is very different from the
672 obtained in Euville stone, being less resistant, especially in compression strength; Alt
673 mortar is the only one with higher flexural and compression strength values close to
674 those of Euville stone.

675 The low open water porosity values of Lit mortar and the slightly higher values
676 obtained through mercury porosity compared to water porosity can be explained by the
677 hydrophobic characteristics of this mortar. Among other reasons, such as the content of
678 clays in its composition, the possible presence of a water-repellent product in the mortar
679 composition could explain crack formation, observed both at the interface of stone-
680 mortar repaired areas at the Grand Palais building. Besides, in the case of these Lit
681 mortar specimens, also a smooth coating is observed on the surface. This surface
682 coating, 'skin' or 'scum' is known as laitance and is formed when fine lime particles
683 held in suspension migrate to the outer surface of the wet material. This laitance is
684 believed to hinder the vapour permeability of lime-based materials, and negatively
685 impact upon the substrate beneath by causing accelerated masonry decay associated
686 with entrapment of moisture. Therefore, it is recommended to remove this laitance from
687 this type of restoration mortar, especially when applied to permeable substrates [9].

688 From the results of the mechanical properties, especially flexural strength, in the case of
689 Alt and Lit mortars and Euville stone it depend, on the apparent density of the material,
690 which is a function of porosity and bulk (mineral) density. C_2S phases, such as larnite,
691 and the carbonation process provide strength in a longer term, while limestone
692 aggregates also increase strength, due to the calcite syntaxial growth, which develops
693 strength thereby enhancing the binder–aggregate interface [13]. This can explain the
694 highest strength values in Alt mortar specimens with higher content in these mineral
695 phases.

696 Regarding to spectrophotometry results, the highest total colour difference (ΔE^*)
697 between each mortar and Euville stone is obtained in Art mortar (circa 8), followed by
698 Alt (circa 5) and Lit mortar that shows the lowest differences (circa 3). According to
699 suitability criteria used to assess conservation treatments, ΔE^* values lower than 5

700 according to the standard NORMAL 20/85 [41], and close to 3 according to other authors
701 [42,43], would not be visually detectable by the human eye and it would not
702 significantly affect the colorimetric parameters of the substrate, which only Lit and Alt
703 mortars would fulfil this criteria after 28 days of hardening.
704 Repair mortars used for stone restoration are assumed to be highly compatible with
705 historic materials in terms of physical, chemical and mechanical properties in order to
706 assure the durability of masonry on the long term [3]. In this sense, these characteristics
707 in Alt mortar are closer to those of Euville stone, compared to the other mortars, with
708 the exception of some differences in the hydric properties due to their different pore
709 systems and aesthetic features that should be improved in further restoration works. The
710 obtained results cannot allow us to conclude which is the best mortar to restore Euville
711 stone, and further studies about mortar-stone interactions will be necessary. This work
712 is an essential step on the research concerning the compatibility and the potential
713 durability of mortars and stone in masonry building restoration.

714 **5. Conclusions**

715 The chemical and mineralogical composition of Euville limestone,(mainly composed of
716 calcium carbonate) and all the studied anhydrous hydraulic mortars (NHL, HL)
717 composed by di-calcium silicate (C_2S,larnite/belite), tri-calcium silicate (C_3S, alite),
718 traces of di-calcium alumina silicate (C_3AS, gehlenite) with presence or absence of
719 phyllosilicates (vermiculite, clinochlore and talc) and aerial lime (portlandite) seems to
720 be critical in the chemistry of the 28 days hardened mortars. The mortar containing
721 calcite, portlandite and no phyllosilicates (Altar Pierre) shows better chemical and
722 mineralogical compatibility with the stone.

723 The soluble salts content of the raw anhydrous mortars is negligible. The presence of
724 chlorides and sulfates (gypsum and mixtures of calcium and sodium sulfates) with

minor amounts of nitrates present in mortar samples collected from historic buildings of Paris suggest an origin of salts caused by contamination/pollution coming from past restoration products and environmental pollution.

Regarding to physical compatibility, the mortars containing higher amounts of phyllosilicates (clinochlore and talc) develop cracks on their surfaces or fissures close to the stone-mortar interface, as observed in Lithomex mortar samples collected from Grand Palais building. However, the aesthetical compatibility obtained from the total color difference values between this mortar and the stone indicates that this is not visually detectable by the human eye.

The addition of marble aggregates and 50-micron spherical aluminosilicate particles to Altar Pierre mortar, favoured hydrolyses reactions and produced a lower porosity matrix with closer hydric and mechanical properties to those of the Euville stone compared to the other two mortars. So, the physico-chemical properties of this mortar are closer to those of the stone, with the exception of some differences in the hydric behaviour due to their different pore systems and aesthetic features that should be improved in further restoration works.

Acknowledgements

Thanks to Foundation des Sciences du Patrimoine / LabEx PATRIMA (2014-2015) for founding the project “Durabilité de l’interaction Mortier-Pierre dans le patrimoine architectural” (acronym: Dimppa) that allowed to carry out this research and the postdoctoral contract of Dr. Lopez-Arce. Thanks also to Roland Westphal (Entreprise Lefèvre) for showing us the restoration works carried out at the Grand Palais. Special thanks to Mrs Ch. Garrat from Grand Palais and Mrs Keller from Préfecture de Police for their decisive help during sampling on the monuments. We are also grateful to Lilian Cristofol and technical engineers that helped in sample preparation and SEM-EDS

analyses from the Civil Engineering Dept. Cergy-Pontoise University (UCP) Finally special thanks as well to Isabell Laureat from the Chemistry Dept. of UCP for all her help performing the calibration of the ion chromatography (IC) equipment.

References

[1] J. Válek, Members of RILEM TC-203-RHM, Performance and Repair Requirements for surface repairs, in: HMC2010 conference and TC 203-RHM final workshop, Prague, September 22-24 Rilem Publications s.a.r.l., 2010, pp. 1377-1383.

[2] J. Griswold, S. Uricheck, Loss Compensation Methods for Stone, JAIC 37 (1998) 89–110.

[3] K. Van Balen, E.E. Toumbakari, M.T. Blanco, J. Aguilera, F. Puertas, C. Sabbioni, G. Zappia, C. Riontino, G. Gobbi, Procedure for a mortar type identification, a proposal, in: P. Bartos, C. Groot, J.J. Hughes (Eds.), Proceedings of International RILEM Workshop on Historic Mortars: Characteristics and Tests, Paisley, Scotland, May 12-14, Rilem Publications s.a.r.l. 1999, pp. 63–72 (1999).

[4] C. Groot, G. Ashall, J. Hughes. Report of RILEM TC COM 167: characterisation of old mortars with respect to their repair. RILEM Report 28, RILEM Publications s.a.r.l., France (2004).

[5] J. Ashurst. N. Ashurst, Practical Building Conservation, English Heritage Handbook, Vol.1, Stone masonry, Gower technical Press ltd (1990).

[6] J.J. Hughes, J. Válek, Mortars in historic buildings. A review of the scientific and conservation literature, Historic Scotland, Edinburgh (2003).

[7] P. Lopez-Arce, J. Garcia-Guinea, D. Benavente, L. Tormo, E. Doehne, Deterioration of dolostone by magnesium sulfate salt: An example of incompatible building materials at Bonaval Monastery, Spain. Constr. Build. Mater. 23 (2009) 846-855.

774 [8] I. Papayianni, M. Stefanidou, Strength-porosity relationships in lime-pozzolan
775 mortars. Constr. Build. Mater. 20 (2006) 700–705.
776 [9] C. Torney, A.M. Forster, P.F.G. Banfill, E.M. Szadurski, The effects of site practice
777 on the physical properties of proprietary stone restoration mortar. Constr Build Mater 75
778 (2015) 359–367.
779 [10] A. Isebaert, L. Van Parys, V. Cnudd, Composition and compatibility requirements
780 of mineral repair mortars for stone – A review. Constr. Build. Mater. 59 (2014) 39–50.
781 [11] B. Szemerey-Kiss, A. Török, Time-dependent changes in the strength of repair
782 mortar used in the loss compensation of stone. Environ Earth Sci. 63 (2011) 1613–1621.
783 [12] V. Rahhal, R. Talero, Effect of three natural pozzolans on portland cement
784 hydration, Mater. Construcc. 53 (2003) 29-40.
785 [13] J. Lanas, J.L. Perez Bernal, M.A. Bello, J.I. Alvarez Galindo, Mechanical
786 properties of natural hydraulic lime-based mortars. Cem. Concr. Res. 34 (2004) 2191–
787 2201.
788 [14] K. Callebaut, J. Elsen, K. Van Balen, W. Viaen, Nineteenth century hydraulic
789 restoration mortars in the Saint Michael's Church (Leuven, Belgium) Natural hydraulic
790 lime or cement? Cem. Concr. Res. 31 (2001) 397-403.
791 [15] J.M. Teutonico, G. Ashall, E. Garrod, T. Yates, A comparative study of hydraulic
792 lime-based mortars, in: P. Bartos, C. Groot, J.J. Hughes (Eds.), Proceedings of
793 International RILEM Workshop on Historic Mortars: Characteristics and Tests, Paisley,
794 Scotland, May 12-14, Rilem Publications s.a.r.l. 1999, pp. 339–349 (1999).
795 [16] L. Schueremans, Ö. Cizer, G. Serré, K.V. Balen, Characterization of repair
796 mortars for the assessment of their compatibility in restoration projects: Research and
797 practice, Constr. Build. Mater. 25 (2011) 4338–4350.

798 [17] D. Gulotta, S. Goidanich, C. Tedeschi, T.G. Nijland, L. Toniolo, Commercial
799 NHL-containing mortars for the preservation of historical architecture. Part 1:
800 Compositional and mechanical characterisation, Cem. Concr. Res. 38 (2013) 31–42.
801 [18] C. Pelosi, U. Santamaria, G. Agresti, G. De Vivo, D. Bandera, Analysis and
802 laboratory tests to evaluate the composition and the behaviour of some dehumidifying
803 mortars used in the restoration field, Periodico di Mineralogia, 82 (2013) 557-572.
804 [19] T. De Kock, J. Dewanckele, M. Boone, G. de Schutter, P. Jacobs, V. Cnudde,
805 Replacement stones for Lede stone in Belgian historical monuments, in: J. Cassar, M.G.
806 Winter, B.R. Marker, N.R.G. Walton, D.C. Entwisle, E.N. Bromhead, J.W.N. Smith
807 (Eds.), Stone in Historic Buildings: Characterization and Performance, Geological
808 Society, London, Special Publications 391, 2014, pp. 31-46.
809 [20] J. Dewanckele, T. De Kock, G. Fronteau, H. Derluyn, P. Vontobel, M. Dierick, L.
810 Van Hoorebeke, P. Jacobs, V. Cnudde, Neutron radiography and X-ray computed
811 tomography for quantifying weathering and water uptake processes inside porous
812 limestone used as building material, Mater. Charact. 88 (2014) 86-99.
813 [21] EN 12620 + A1:2008 (2002) Aggregates for Concrete.
814 [22] AFNOR EN 196-1 (2006) Méthodes d'essai des ciments Partie 1: Détermination de
815 la résistance mécaniques, France.
816 [23] AFNOR EN 1015-11, Méthodes d'essai des mortiers pour maçonnerie. Partie 11:
817 Détermination de la résistance en flexion et en compression du mortier durci, France
818 2000.
819 [24] A. Arizzi, G. Martínez- Huerga, E. Sebastian-Pardo, G. Cultrone, Mineralogical,
820 textural and physical-mechanical study of hydraulic lime mortars cured under different
821 moisture conditions, Mater. Construcc. 65 (2015).

822 [25] A. Arizzi, H. Viles, G. Cultrone, Experimental testing of the durability of lime-
823 based mortars used for rendering historic buildings, Constr. Build. Mater. 28 (2012)
824 807-818.
825 [26] AFNOR NF-EN 1015-1(P12-301), Méthodes d'essai des mortiers pour
826 maçonnerie. Partie 1: Détermination de la répartition granulométrique (par tamisage),
827 France, 1999.
828 [27] AFNOR EN 1925, Méthodes d'essai pour Pierres naturelles Détermination du
829 coefficient d'absorption d'eau par capillarité, France, 1999.
830 [28] AFNOR EN 15803, Méthodes d'essai : détermination de la perméabilité à la
831 vapeur d'eau, France, 2010.
832 [29] AFNOR EN 1936, Méthodes d'essai des Pierres naturelles maçonnerie :
833 Détermination des masses volumiques réele et apparentes et des porosités ouverte et
834 totale, France, 2007.
835 [30] AFNOR EN 196-1, Méthodes d'essai des ciments Partie 1: Détermination de la
836 résistance mécaniques, France, 2006.
837 [31] P. Lopez-Arce, M. Tagnit-Hammou, B. Menendez, J-D. Mertz, A. Kaci, Durability
838 of stone-repair mortars used in historic buildings from Paris, Materials and Structures,
839 DOI 10.1617/s11527-016-0846-0
840 [32] B. Menendez, J.D. Mertz, M. Guiavarc'h, A. Kaci, S. Aggoun, P. Lopez-Arce,
841 Durabilité de l'interaction Mortier-Pierre dans le patrimoine architectural (acronym:
842 Dimppa project). Foundation des Sciences du Patrimoine / LabEx PATRIMA (2014-
843 2015), Final technical report.
844 [33] F. Winnefeld, K.G. Böttger, How clayey fines in aggregates influence the
845 properties of lime mortars. Mater. Struct. 39 (2006) 433-443.

[34] P. Maravelaki-Kalaitzaki, A. Bakolas, I. Karatasios, V. Kilikoglou, Hydraulic lime mortars for the restoration of historic masonry in Crete, Cem. Concr. Res. 35 (2005) 1577– 1586.

[35] A. Moropoulou, A. Bakolas, K. Bisbikou, Physico-chemical adhesion and cohesion bonds in joint mortars imparting durability to the historic structures, Constr. Build. Mater. 14 (2000) 35–46.

[36] A. Moropoulou, A. Bakolas, K. Bisbikou, Investigation of the technology of historic mortars, J. Cult. Herit. 1 (2000) 45– 58.

[37] A. Moropoulou, G. Biscontin, A. Bakolas, K. Bisbikou, Technology and behavior of rubble masonry, Constr. Build. Mater. 11 (1997) 119–129.

[38] E.P. Mora, J. Paya, J. Monzo, Influence of different sized fractions of a fly ash on workability of mortars. Cem. Concr. Res. 23 (1993) 917–924.

[39] L.J. Malvar, L.R. Lenke, Efficiency of fly ash in mitigating alkali silica reaction based on chemical composition, ACI Mater. J. 103 (2006) 319–326.

[40] E. Pecchioni, P. Malesani, B. Bellucci, F. Fratini, Artificial stones utilised in Florence historical palaces between the XIX and XX centuries, J. Cult. Herit. 6 (2005) 227–233.

[41] NORMAL 20/85, Interventi conservativi: progettazione esecuzione e valutazione preventive, Italy, 1986.

[42] D. Benavente, F. Martinez-Verdu, A. Bernabeu, V. Viqueira, R. Fort, M.A. Garcia del Cura, C. Illueca, S. Ordoñez, Color Res. Appl. 28 (2003) 343–351.

[43] J.D. Rodrigues, A. Grossi, Indicators and ratings for the compatibility assessment of conservation actions, J. Cult. Herit. 8 (2007) 32–43.

FIGURE CAPTIONS

Figure 1. Mortar and stone materials. a) Raw anhydrous ready to mix mortars (left: *Lit* mortar; center: *Alt* mortar; right: *Art* mortar); b) Euville stone specimen used for water vapour permeability test; c) 28 days hardened mortars specimens (Left: *Lit* mortar; center: *Alt* mortar; right: *Art* mortar) after capillarity water absorption test.

Figure 2. Mortar and stone samples collected from historic buildings of Paris. a) Lit mortar from Grand Palais building; b) Alt mortar from Préfecture Police building; c) Euville stone flake from Préfecture Police.

Figure 3. X-ray diffraction patterns (XRD) of the raw anhydrous mortars (Lit: Lithomex; Art: ArtoPierre;. Alt: Altar Pierre)

Figure 4. SEM-EDS analyses performed in several areas of mineral grains with sizes between 1.6-1.25 mm and 1.25 mm-0.63 mm of Lithomex (Litho, Lit), ArtoPierre (Arto, Art) and Altar Pierre (Altar, Alt) mortars. a) phyllosilicates (clinochlore and talc), with and without additional K, Ti and Cl with sizes between 1.6-1.25 mm in Lit mortar; b) calcite grains (1.25 mm-0.63 mm) in Lit mortar; c) phyllosilicates (1.25-063 mm) in Art mortar; d) calcite grains (1.25 mm-0.63 mm) in Alt mortar.

Figure 5. Thin sections obtained by light optical microscopy in mortar samples collected from historic buildings of Paris. a) Lit mortar from Grand Palais building (Lit-GP); b) same former image with crossed nicols; c) Lit mortar, detail of fissural porosity (in blue); d) same former image with crossed nicols; e) Alt mortar from Préfecture Police building (Alt-PP); f) same former image with crossed nicols; g) Alt mortar, detail of same sample showing porosity (in blue).

Figure 6. X-ray diffraction pattern of mortar samples collected from historic buildings of Paris. Lit-GP (Lithomex mortar from Grand Palais); Alt -PP (Altar Pierre from Préfecture Police); Lit-GP-sf (evaporated soluble fraction together with non-soluble residues).

Figure 7. Scanning electron microscopy (SEM) images and energy dispersive spectroscopy (EDS) analyses performed on the surface of mortar and stone samples collected from historic buildings of Paris. a) Lit mortar from the Grand Palais; b) Alt mortar from Préfecture de Police; c) efflorescences in Euville stone flake from Préfecture de Police.

Figure 8. Connected porosity and pore size distribution obtained by mercury intrusion porosimetry in mortar samples collected from historic buildings of Paris. a) Lit mortar from Grand Palais; b) Alt mortar from Préfecture de Police.

Figure 9. Thin sections observed by light optical microscopy of the 28 days hardened mortars manufactured in the lab and of Euville stone. a) Lit mortar with parellel nicols; b) same former image with crossed nicols; c) Alt mortar with parellel nicols; d) same former image with crossed nicols; e) Art mortar with parellel nicols; f) same former image with crossed nicols; g) Euville stone with parellel nicols; h) same former image with crossed nicols.

Figure 10. X-ray diffraction pattern of 28 days (28d) hardened mortars manufactured in the laboratory (Lit: Lithomex mortar; Art: Artopierre mortar; Alt: Altar Pierre mortar).

Figure 11. Representation of hydric properties of 28 days hardened mortars and stone specimens. a) capillarity water absorption of mortars; b) water desorption (water loss) of mortars; c) capillarity water absorption of Euville stone; d) water desorption (water loss) of Euville; e) water vapor permeability of mortars; f) water vapor permeability of Euville stone.

Figure 12. Connected porosity and pore size distribution obtained by mercury intrusion porosimetry in 28 days hardened mortars and Euville stone.

Table 1. Semi-quantitative (%) X-ray diffraction (XRD) analyses of the raw anhydrous and 28 days hardened mortars together with mortar samples from historic buildings from Paris

Mortar	Calcite	Quartz	Feldspar	Gypsum	Clinochlore	Talc	Dolomite	Muscovite	C_3S	C_2S	C_2AS	CH	halite
Lit-raw	20	10	5	Nd*	10	45	traces	Nd*	5	5	traces	Nd*	Nd*
Art-raw	15	50	traces	Nd*	Nd*	Nd*	Nd*	Nd*	5	10	traces	20	Nd*
Alt-raw	20	35	15	traces	Nd*	Nd*	Nd*	Nd*	5	10	traces	15	Nd*
Lit-GP*	14	14	10	5	21	20	Nd*	16	Nd*	Nd*	traces	Nd*	Nd*
Lit-GP-$_{sf*}$	15	5	Nd*	8	49	18	Nd*	Nd*	Nd*	Nd*	Nd*	Nd*	5
Alt-PP	15	60	14	Nd*	Nd*	Nd*	Nd*	Nd*	Nd*	6	traces	5	Nd*
Lit-28D	20	21	5	Nd*	26	28	Nd*	Nd*	Nd*	traces	Nd*	Nd*	Nd*
Art-28D	20	61	9	Nd*	traces	Nd*	Nd*	Nd*	Nd*	5	traces	5	Nd*
Alt-28D	18	50	20	Nd*	Nd*	Nd*	Nd*	Nd*	traces	6	traces	6	Nd*

*Nd: No detected; Lit: Lithomex mortar; Alt: Altar Pierre mortar; Art: ArtoPierre mortar; raw: anhydrous raw mortar; GP: Grand Palais building; PP: Préfecture Police building; sf: evaporated soluble fraction; 28D: 28 days hardened mortar; C_2S: Di-calcium silicate, Ca_2SiO_4 (larnite/belite); C_3S: Tri-calcium silicate, Ca_3SiO_5 (alite); CH: Calcium hydroxide (portlandite); C_2AS: gehlenite

Table 2. Qualitative elemental analyses performed by punctual energy dispersive spectroscopy (SEM-EDS) on several grains of the largest grain size fractions (aggregates) of the raw anhydrous mortars embedded in epoxy resin.

Mortar	Lit mortar		Art mortar		Alt mortar	
Grain size interval	1.60-1.25mm	1.25-0.63mm	1.60-1.25mm	1.25-0.63mm	1.60-1.25mm	1.25-0.63mm
Normalized wt.%						
Ca	Present	Present	Present	Present	Present	Present
Si	Present	Present	Present	Present	Present	Present
Al	Present	Present	Present	Present	No detected	No detected
Mg	Present	Present	Present	Present	No detected	No detected
O	Present	Present	Present	Present	Present	Present
C	Present	Present	Present	Present	Present	Present
K	Present	No detected	Present	Present	No detected	No detected
Na	Present	Present	Present	No detected	Present	No detected
Fe	Present	Present	Present	Present	No detected	Present
Ti	Present	No detected	Present	Present	No detected	Present
Cl	Present	No detected	Present	Present	Present	Present

Table 3. Semi-quantitative (%) energy dispersive spectroscopy (EDS) analyses performed on the finest grain size fractions (aggregates and binder) of the raw anhydrous mortars pressed on tablets.

Grain size	0.63-0.315 mm			0.315-0.20 mm			0.20-0.16 mm			0.16-0.080 mm			<0.080 mm		
Mortar	Lit	Art	Alt	Lit	Art	Alt	Lit	Art	Alt	Lit	Art	Alt	Lit	Art	Alt
Normalized wt.%															
Ca	13.1	19.7	3.8	11.0	11.3	5.4	9.3	38.3	27.0	7.5	32.6	28.3	3.9	39.7	33.0
Si	19.2	23.0	39.0	20.7	33.1	41.2	11.0	8.0	6.3	5.2	5.5	5.6	8.0	2.4	6.3
Al	0.5	0.4	1.1	0.6	0.6	1.5	0.8	0.4	1.4	1.2	0.5	1.7	1.9	0.5	1.8
Mg	0.5	0.5	0.2	0.4	0.4	0.2	1.2	0.4	1.8	4.8	0.5	2.2	7.7	0.5	1.8
O	52.3	45.6	50.8	50.7	48.0	48.0	59.8	46.7	54.8	61.8	52.5	54.0	61.9	49.1	50.2
C	12.6	10.8	4.6	14.7	6.2	2.5	17.6	5.8	7.1	19.3	7.4	7.3	16.1	7.3	6.0
S	0.0	0.0	0.0	0.0	0.0	0.0	0.0	0.4	1.0	0.3	0.4	0.7	0.4	0.4	0.8
K	0.2	0.0	0.8	0.2	0.4	1.2	0.0	0.2	0.1	0.0	0.2	0.0	0.0	0.1	0.0
Na	0.0	0.0	3.8	0.0	0.0	5.4	0.0	0.0	27.0	0.0	0.4	0.4	0.0	0.0	33.0

*Lit: Lithomex mortar; Art: Artopierre mortar; Alt: Altar Pierre mortar

Table 4. Soluble salt content determined by ion chromatography analyses of the raw anhydrous mortars

Soluble salts		Anions (ppm)				Cations (ppm)					Wt.
Samples		Cl^-	SO_4^{2-}	NO_3^-	PO_4^{3-}	Na^+	NH_4^+	K^+	Mg^{2+}	Ca^{2+}	(%)
anhydrous mortar	Lit	5	23	0	0	22	0.00	3	1	129	2
	Art	5	0	0	0	16	0.00	3	1	534	5
	Alt	6	0	0	0	22	0.00	3	3	165	2

933 **Table 5**. Soluble salt content determined by ion chromatography analyses of mortar and stone samples collected from Grand

934 Palais (GP) and Préfecture Police (PP) buildings.

Soluble salts		Anions (ppm)				Cations (ppm)					wt.
Samples		Cl^-	SO_4^{2-}	NO_3^-	PO_4^{3-}	Na^+	NH_4^+	K^+	Mg^{2+}	Ca^{2+}	(%)
Mortar From buildings	Lit-GP	30	105	25	0	22	0	9	5	97	3
	Alt-PP	12	21	34	0	17	0	2	2	15	1
Stone flake	EU-PP	17	984	0	0	58	0	152	7	261	13

935

936 **Table 6**. Results from hydric characterization of 28 days hardened mortars and stone specimens

Properties / samples	Lit mortar	Art mortar	Alt mortar	Euville stone
Capillary Coefficient ($g/m^2.s^{0.5}$)	11.63	73.85	43.20	45.60
Desorption Coefficient ($g/m^2.s^{0.5}$)	-5.16	-29.41	-7.79	-49.80

Water vapour permeability Kg/ (m.s.Pa)	3.08E-11	4E-11	1.79E-11	1.57E-11
Open porosity (%)	31.1 ± 1.1	39.1 ± 1.0	25.0 ± 0.2	16.5 ± 1.0
Apparent density (g/cm^3)	1.67 ± 0.00	1.58 ± 0.01	1.88 ± 0.03	2.25 ± 0.02
Bulk density (g/cm^3)	2.45 ± 0.04	2.59 ± 0.00	2.51 ± 0.01	2.69 ± 0.01

937

938 **Table 7**. Mercury intrusion porosimetry results obtained in 28 days hardened mortars and stone

Properties / samples	Lit mortar	Art mortar	Alt mortar	Euville stone
Porosity (%)	32.24	31.77	21.13	14.92
Apparent density (g/cm^3)	1.69	1.57	1.88	2.17
Bulk density (g/cm^3)	2.49	2.30	2.38	2.55
Average pore radius (µm)	0.10	0.13	0.04	1.47
Median pore radius (µm)	0.48	0.41	0.01	0.82
Mode pore radius (µm)	0.76	0.95 (0.28)	0.34 (0.25)	0.60

939

940 **Table 8.** Flexural and compression strength of 28 days hardened mortars and Euville stone.

Strength (MPa)	Lit mortar	Art mortar	Alt mortar	Euville stone
Flexural	3.91 ± 0.05	2.22 ± 0.08	4.22 ± 0.16	4.84 ± 0.35
Compression	9.01*	<7	15.65 ± 2.88	27.07 ± 5.25

941 * In the other specimens compression was <7

942 **Table 9.** Colour parameters (L*, lightness; a* and b* colour coordinates; C*, Chroma; ΔE*, total colour difference) obtained in

943 28 days hardened mortar specimens and Euville stone.

Material	L*	a*	b*	C* (D65)	Hue (D65)	ΔE*
Lit	78.44± 0.10	2.35 ± 0.02	11.32 ± 0.04	11.56 ± 0.04	78.30 ± 0.06	3.22
Art	88.05± 0.11	0.93 ± 0.03	6.34 ± 0.08	6.47 ± 0.08	81.72 ± 0.13	7.80
Alt	76.36± 0.06	1.60 ± 0.01	9.56 ± 0.03	9.70 ± 0.04	80.50 ± 0.06	5.16
Stone	81.38± 1.09	2.68 ± 0.28	10.06 ± 1.44	10.41 ± 1.45	74.98 ± 1.46	Reference

944

945

946

FIGURE 1

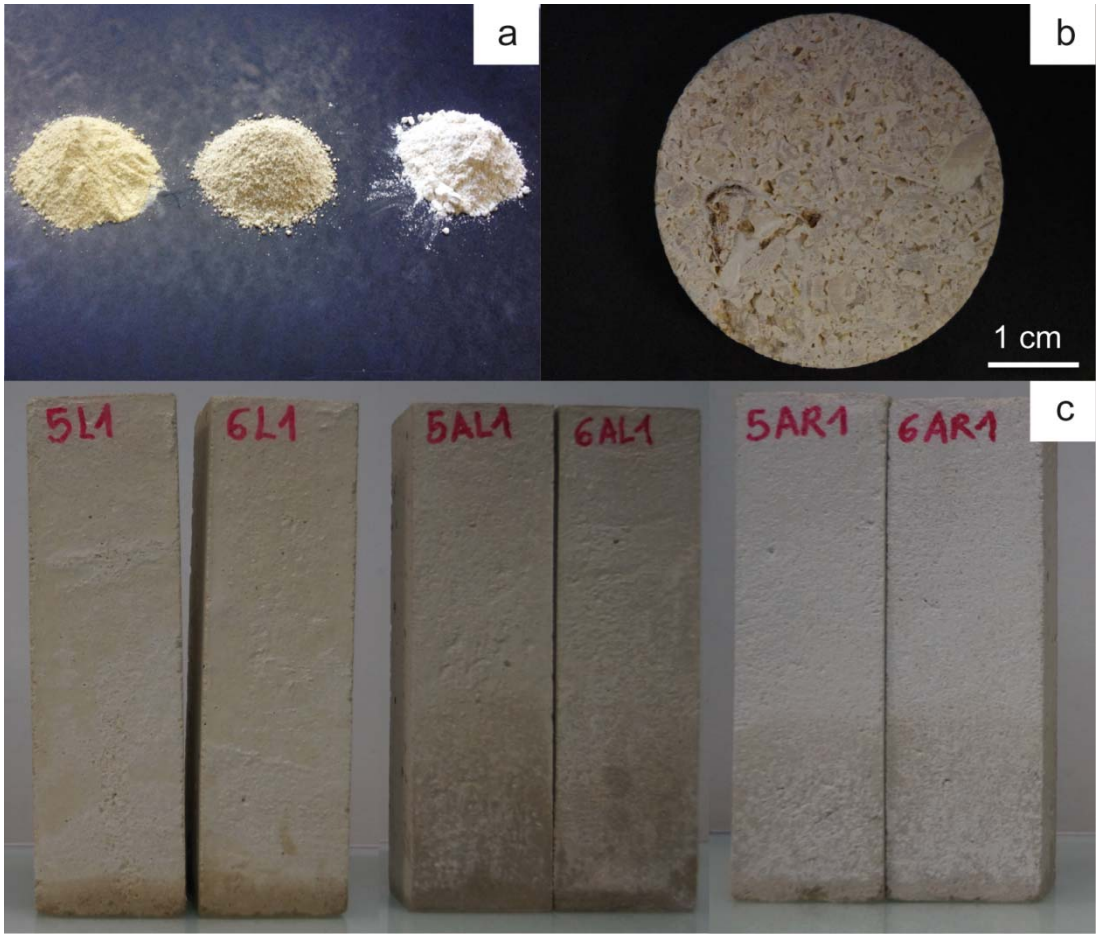

FIGURE 2

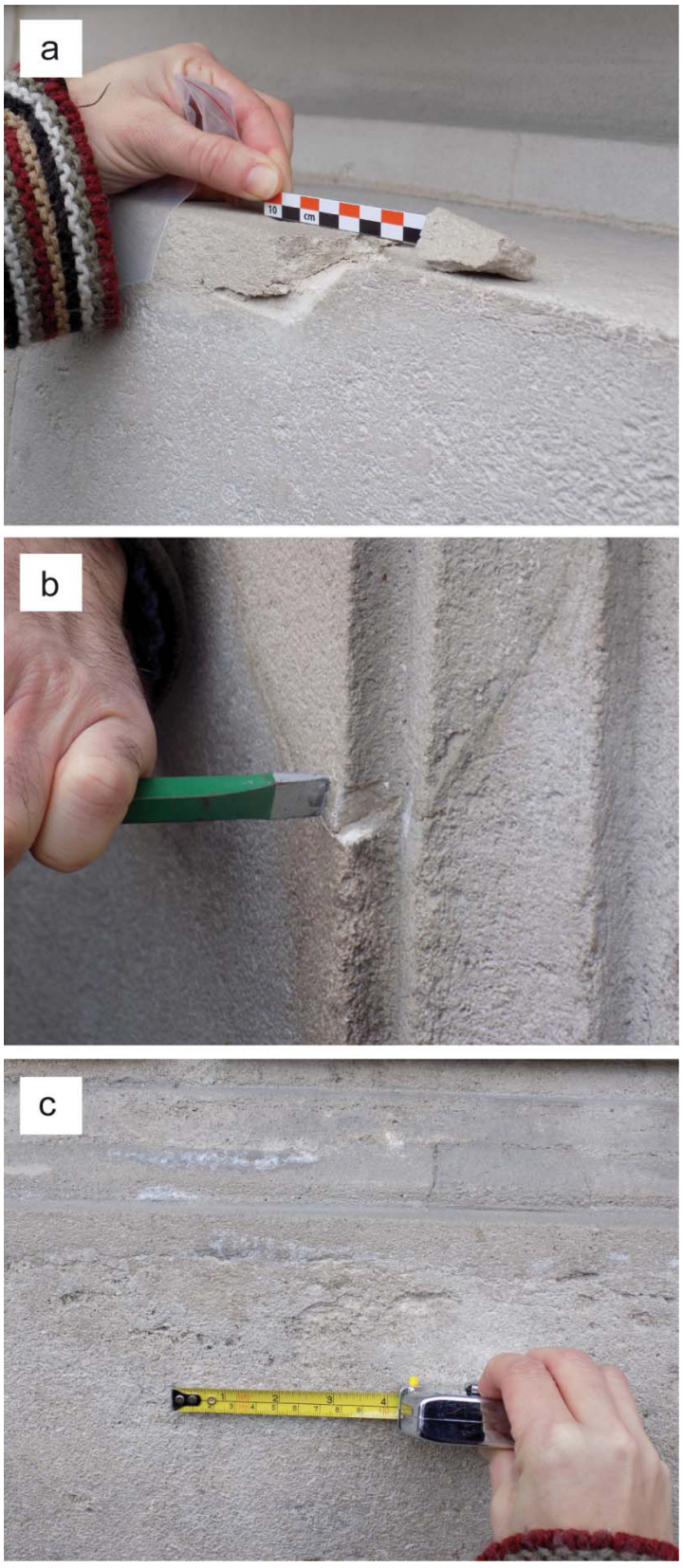

FIGURE 3

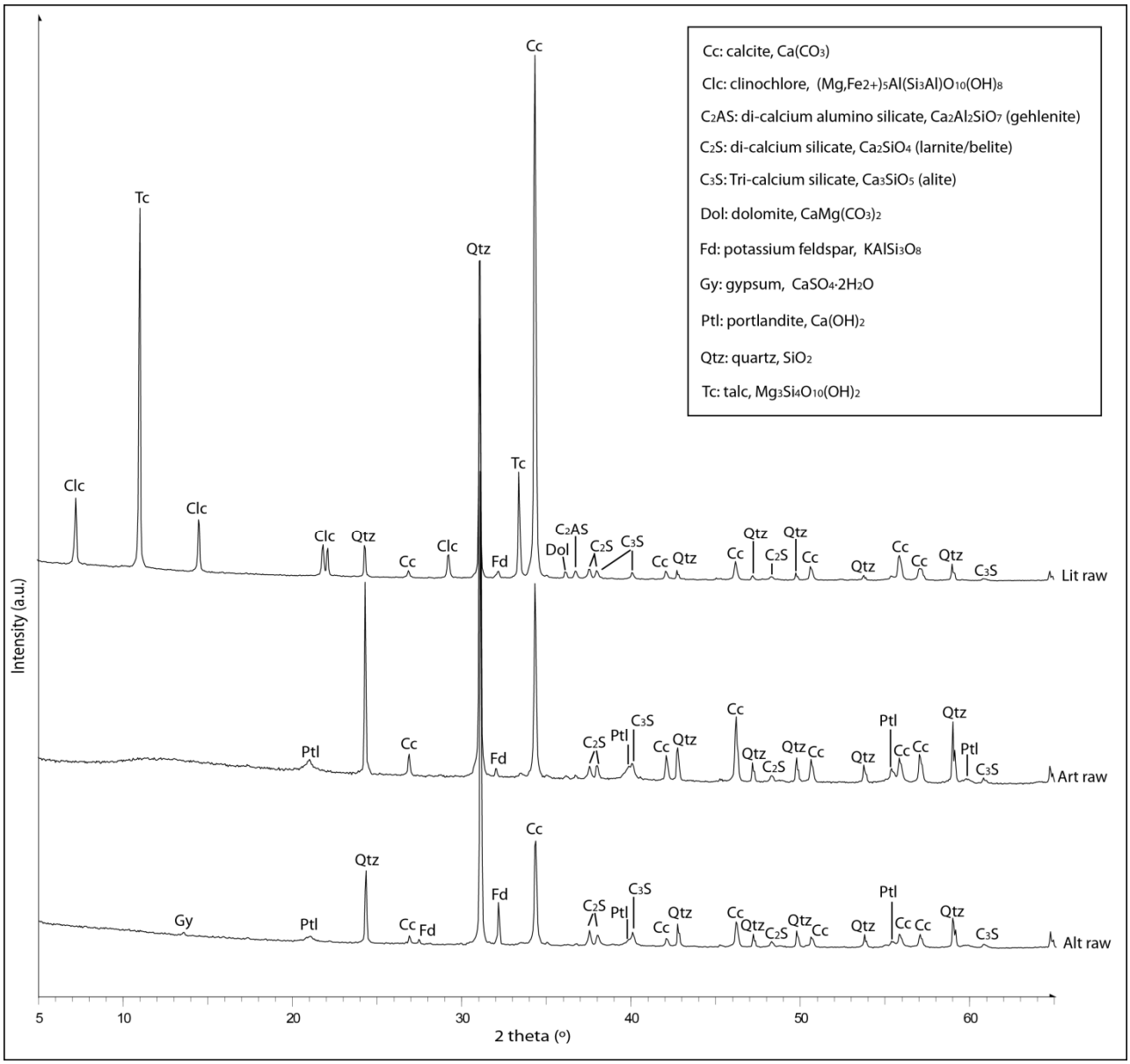
Cc: calcite, Ca(CO3)
Clc: clinochlore, (Mg,Fe2+)5Al(Si3Al)O10(OH)8
C2AS: di-calcium alumino silicate, Ca2Al2SiO7 (gehlenite)
C2S: di-calcium silicate, Ca2SiO4 (larnite/belite)
C3S: Tri-calcium silicate, Ca3SiO5 (alite)
Dol: dolomite, CaMg(CO3)2
Fd: potassium feldspar, KAlSi3O8
Gy: gypsum, CaSO4·2H2O
Ptl: portlandite, Ca(OH)2
Qtz: quartz, SiO2
Tc: talc, Mg3Si4O10(OH)2
Intensity (a.u.)
2 theta (°)
5
10
20
30
40
50
60
Lit raw
Art raw
Alt raw

FIGURE 4

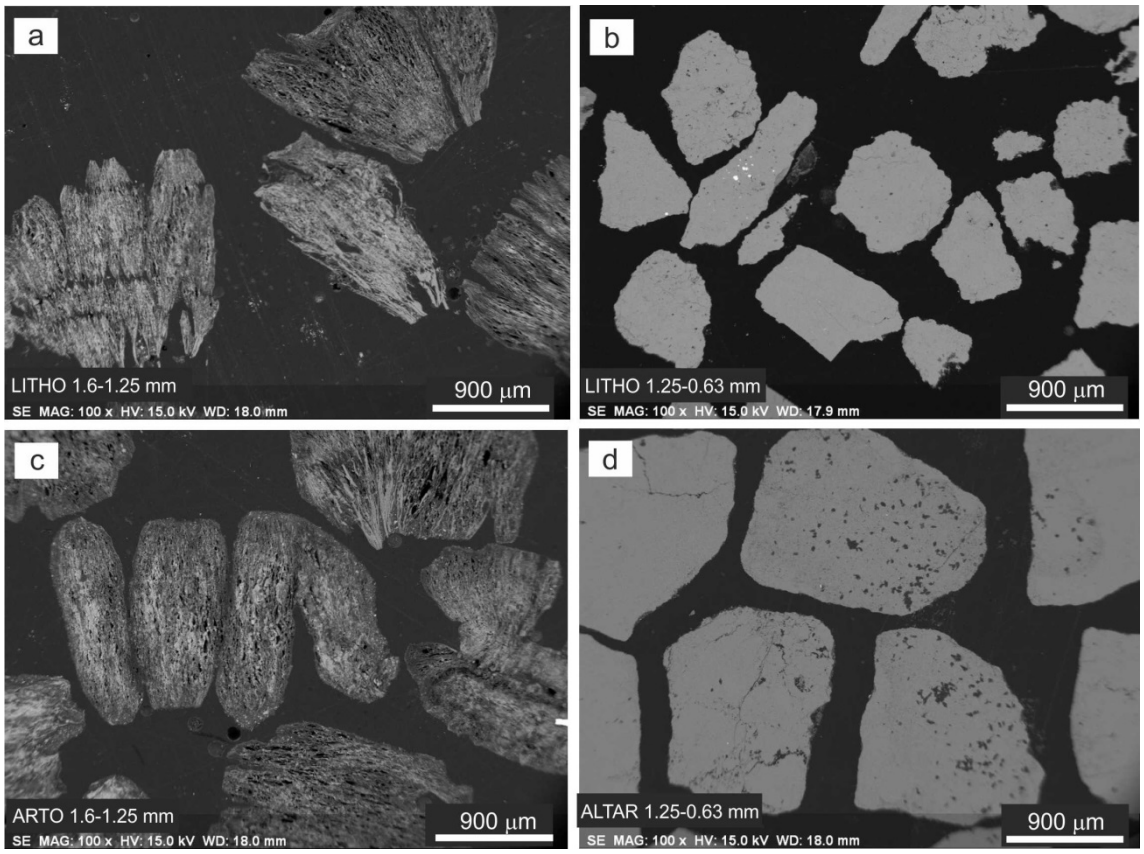
a
LITHO 1.6-1.25 mm
SE MAG: 100 x HV: 15.0 kV WD: 18.0 mm
900 μm
b
LITHO 1.25-0.63 mm
SE MAG: 100 x HV: 15.0 kV WD: 17.9 mm
900 μm
c
ARTO 1.6-1.25 mm
SE MAG: 100 x HV: 15.0 kV WD: 18.0 mm
900 μm
d
ALTAR 1.25-0.63 mm
SE MAG: 100 x HV: 15.0 kV WD: 18.0 mm
900 μm

FIGURE 5

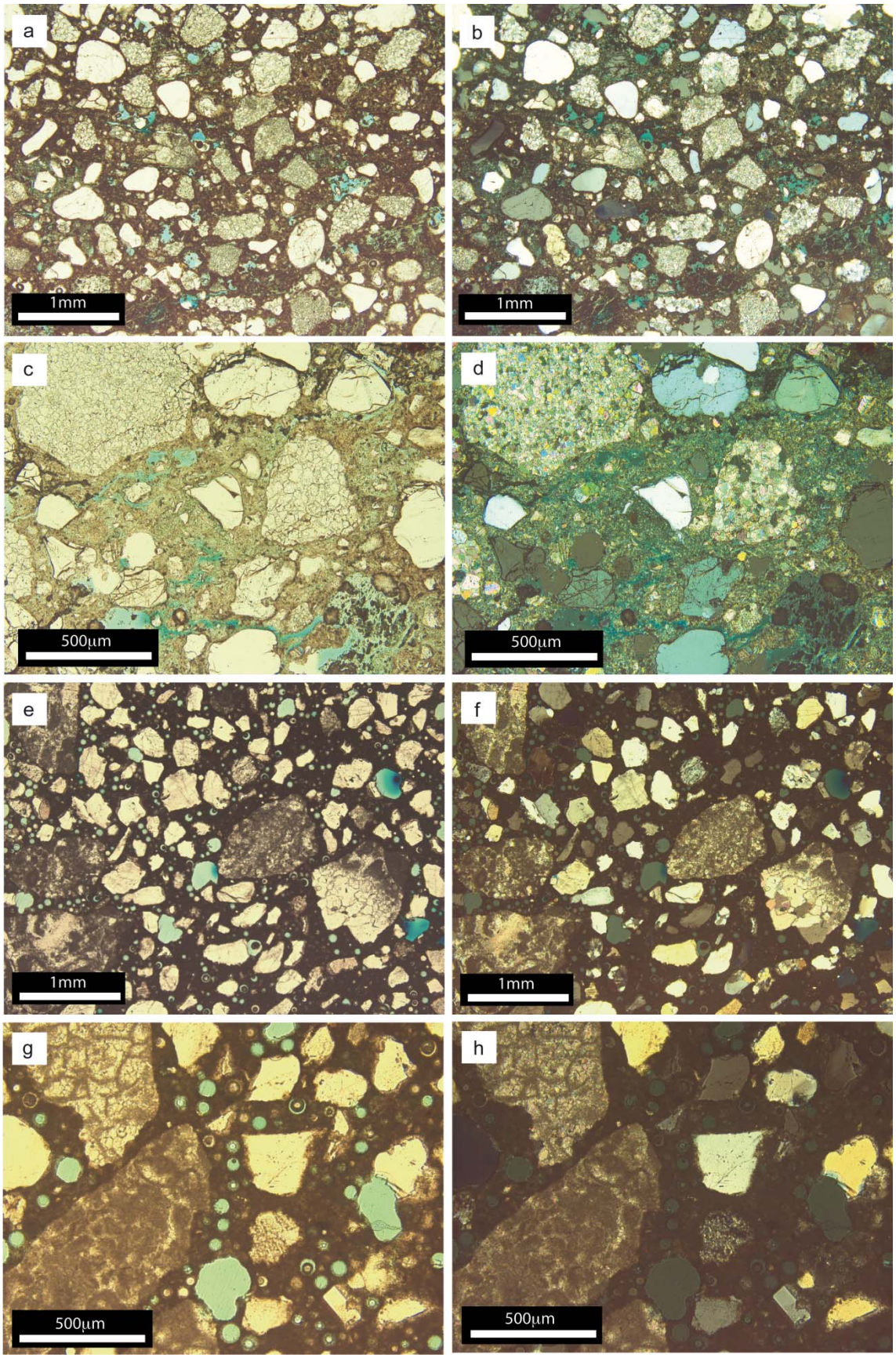

FIGURE 6

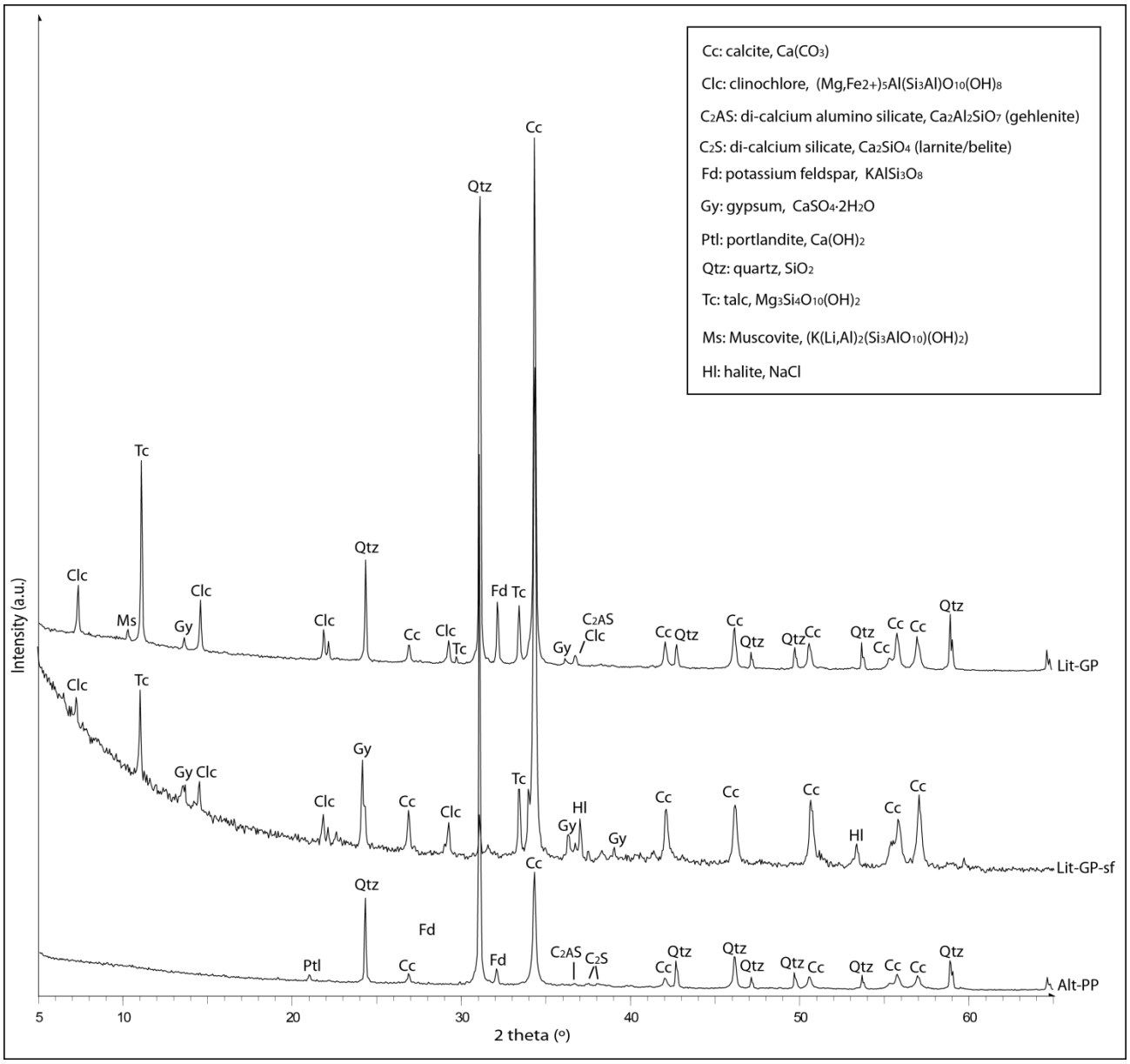
Cc: calcite, Ca(CO3)
Clc: clinochlore, (Mg,Fe2+)5Al(Si3Al)O10(OH)8
C2AS: di-calcium alumino silicate, Ca2Al2SiO7 (gehlenite)
C2S: di-calcium silicate, Ca2SiO4 (larnite/belite)
Fd: potassium feldspar, KAlSi3O8
Gy: gypsum, CaSO4·2H2O
Ptl: portlandite, Ca(OH)2
Qtz: quartz, SiO2
Tc: talc, Mg3Si4O10(OH)2
Ms: Muscovite, (K(Li,Al)2(Si3AlO10)(OH)2)
Hl: halite, NaCl
Intensity (a.u.)
2 theta (°)
Lit-GP
Lit-GP-sf
Alt-PP
5
10
20
30
40
50
60

FIGURE 7

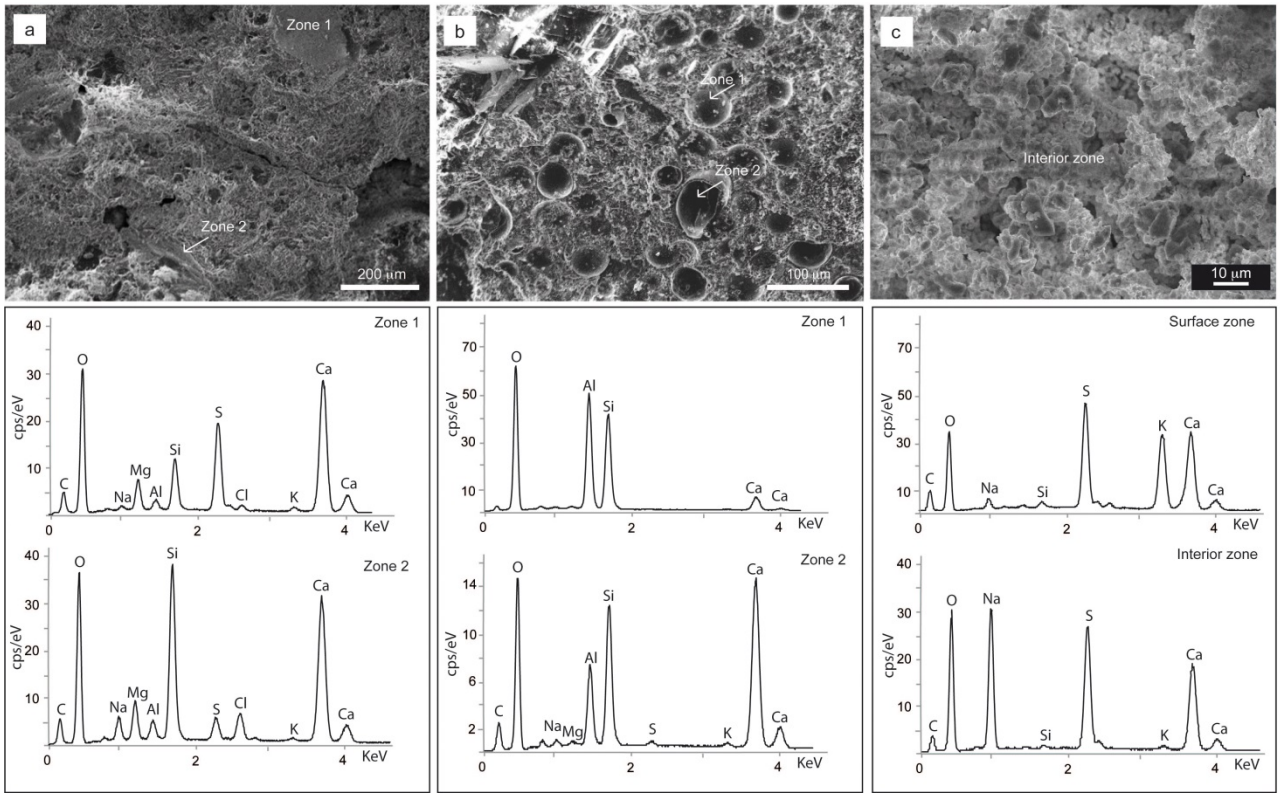

FIGURE 8

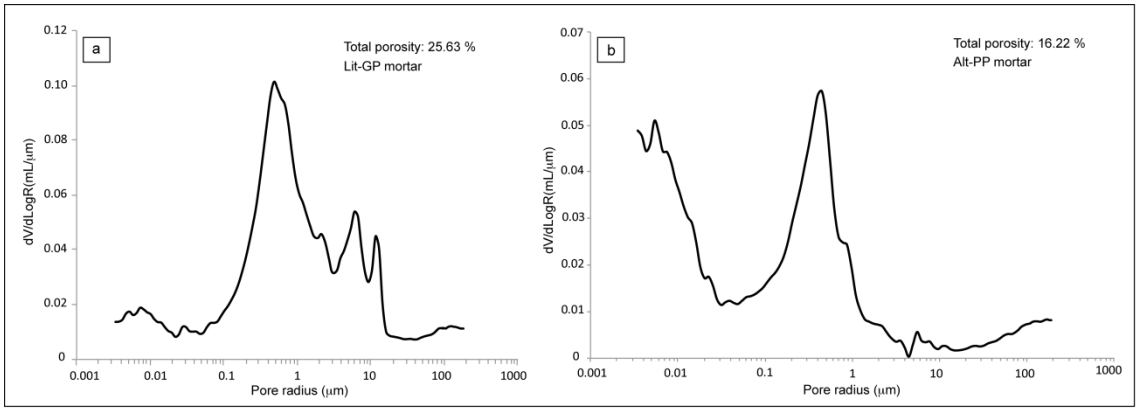

FIGURE 9

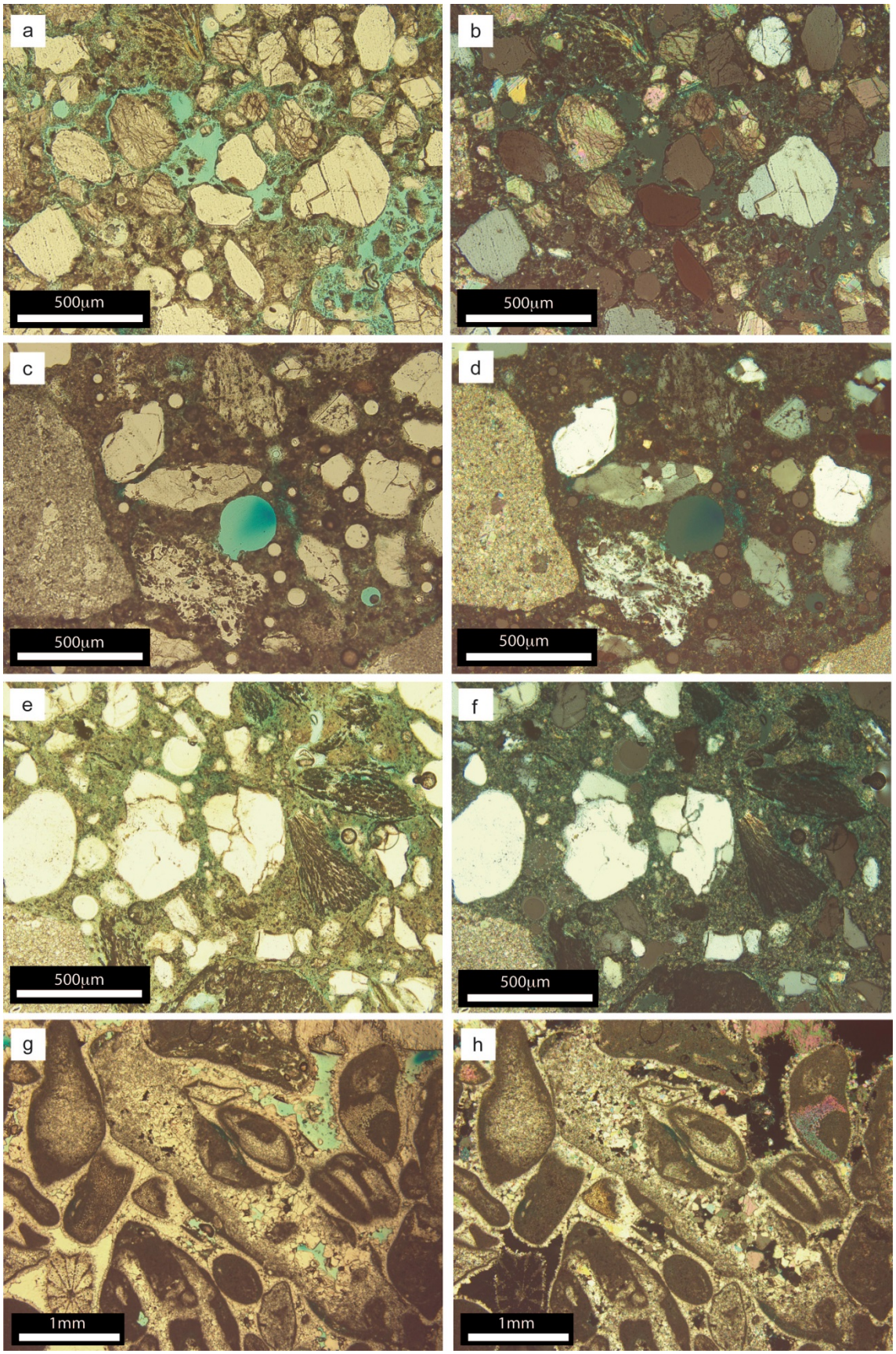

FIGURE 10

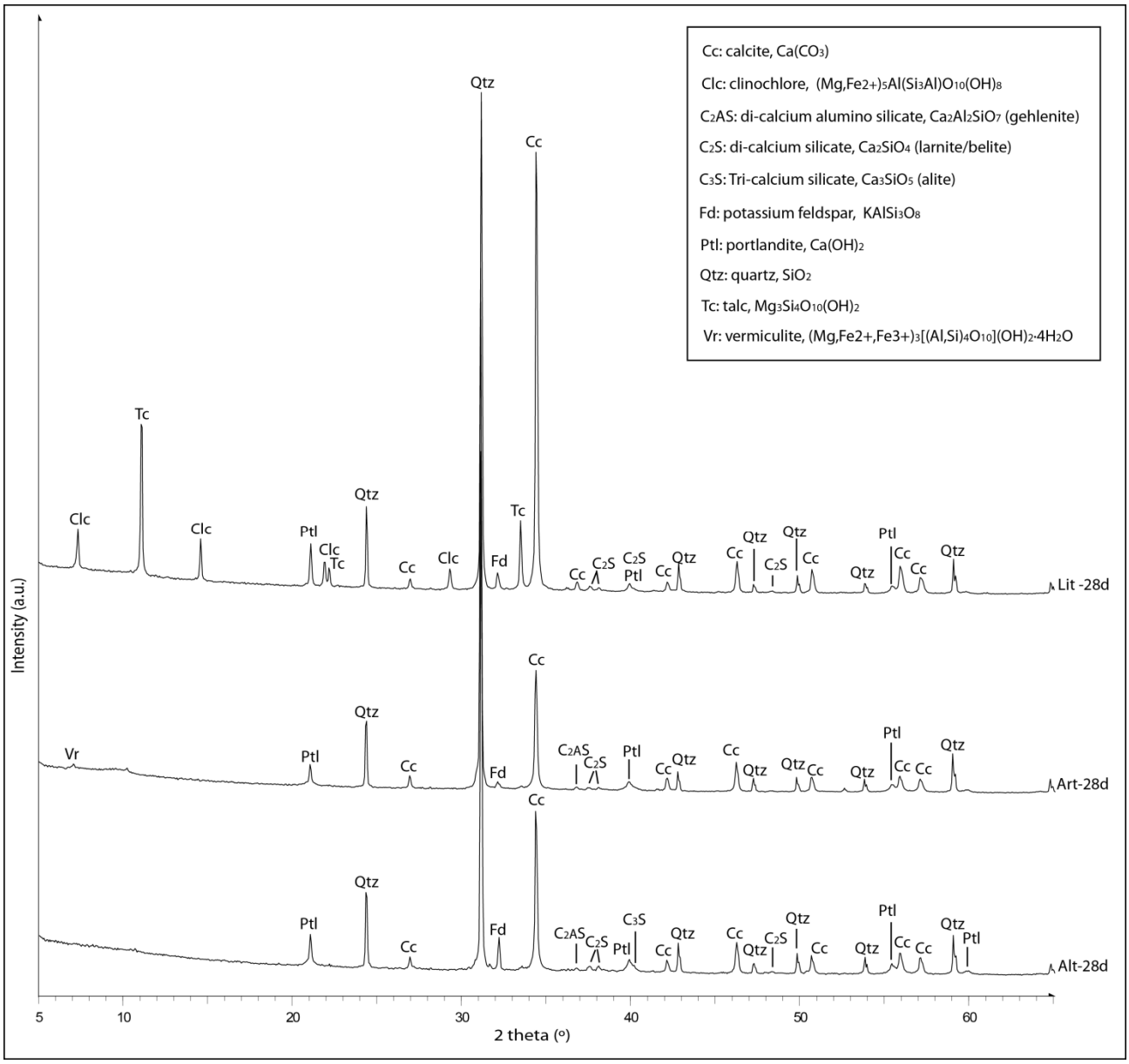
Cc: calcite, Ca(CO3)
Clc: clinochlore, (Mg,Fe2+)5Al(Si3Al)O10(OH)8
C2AS: di-calcium alumino silicate, Ca2Al2SiO7 (gehlenite)
C2S: di-calcium silicate, Ca2SiO4 (larnite/belite)
C3S: Tri-calcium silicate, Ca3SiO5 (alite)
Fd: potassium feldspar, KAlSi3O8
Ptl: portlandite, Ca(OH)2
Qtz: quartz, SiO2
Tc: talc, Mg3Si4O10(OH)2
Vr: vermiculite, (Mg,Fe2+,Fe3+)3[(Al,Si)4O10](OH)2·4H2O
Intensity (a.u.)
2 theta (°)
5
10
20
30
40
50
60
Lit -28d
Art-28d
Alt-28d

FIGURE 11

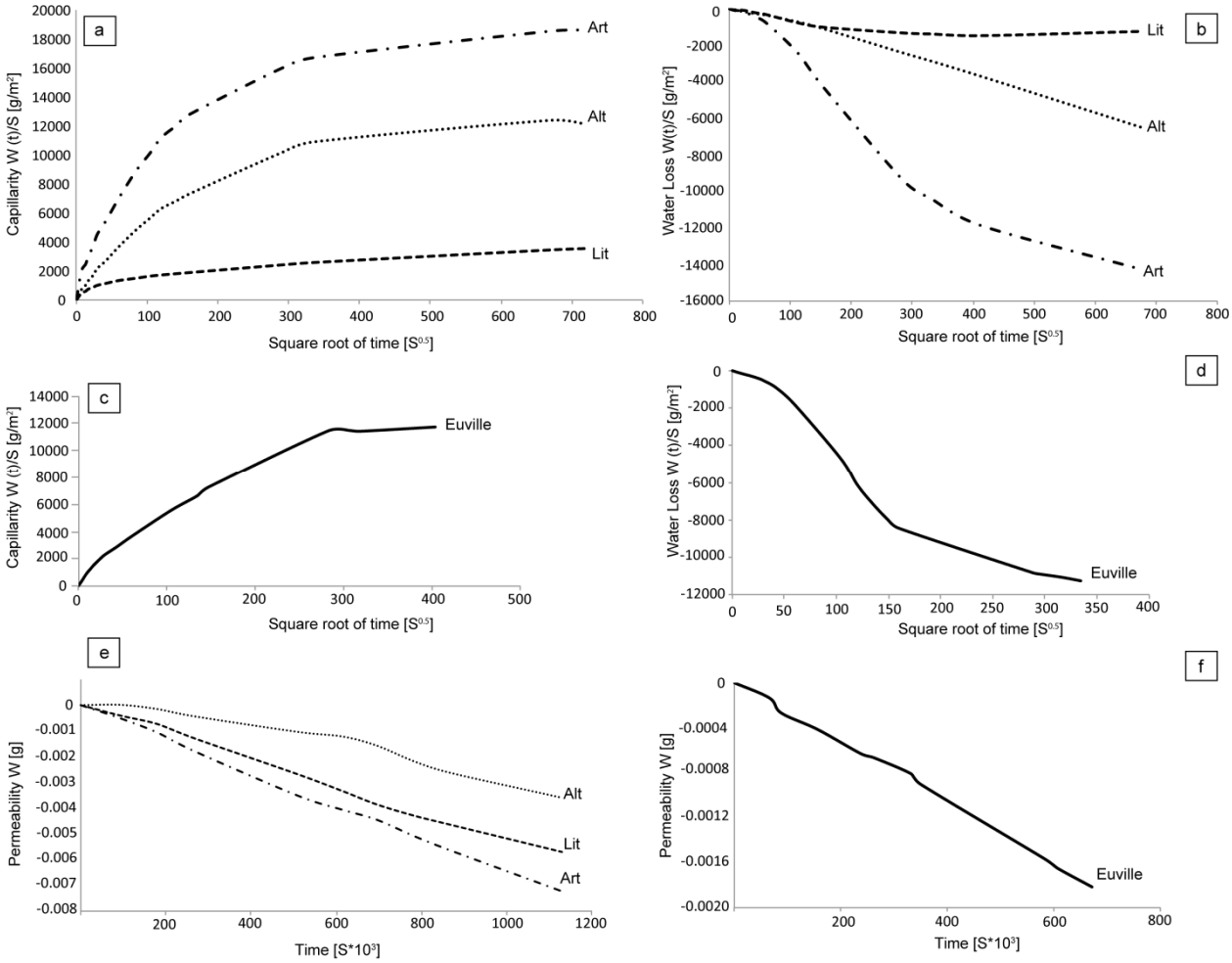
a
Capillarity W (t)/S [g/m²]
Square root of time [S^0.5]
Art
Alt
Lit
b
Water Loss W(t)/S [g/m²]
Square root of time [S^0.5]
Lit
Alt
Art
c
Capillarity W (t)/S [g/m²]
Square root of time [S^0.5]
Euville
d
Water Loss W (t)/S [g/m²]
Square root of time [S^0.5]
Euville
e
Permeability W [g]
Time [S*10³]
Alt
Lit
Art
f
Permeability W [g]
Time [S*10³]
Euville

FIGURE 12

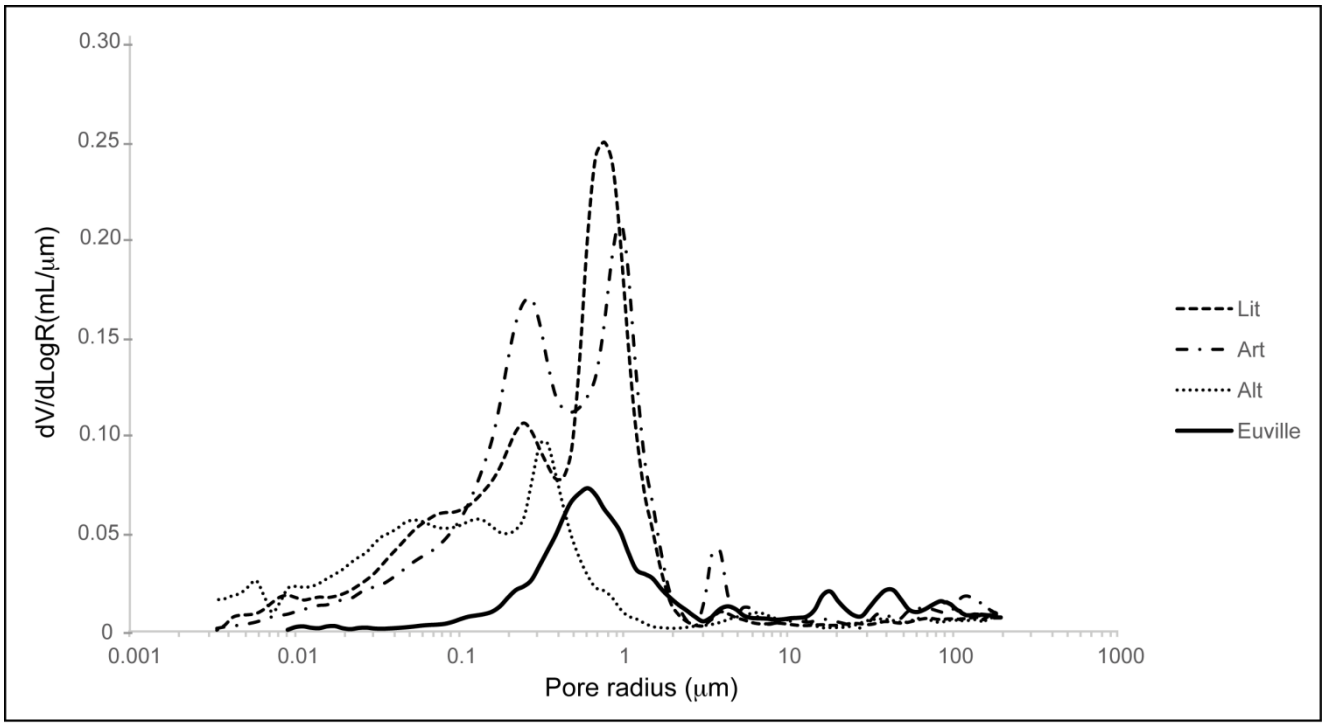
0.30
0.25
0.20
0.15
0.10
0.05
0
dV/dLogR(mL/μm)
0.001
0.01
0.1
1
10
100
1000
Pore radius (μm)
Lit
Art
Alt
Euville